PARTIAL ATTITUDE SYNCHRONIZATION OF UNDERACTUATED SPACECRAFT SYSTEMS

A Thesis
Presented to
The Academic Faculty

by

John Matthew Brewer

In Partial Fulfillment
of the Requirements for the Degree
Master of Science in the
School of Aerospace Engineering

Georgia Institute of Technology
December 2016

PARTIAL ATTITUDE SYNCHRONIZATION OF UNDERACTUATED SPACECRAFT SYSTEMS

Approved by:

Dr. Panagiotis Tsiotras, Advisor
School of Aerospace Engineering
Georgia Institute of Technology

Dr. Marcus Holzinger
School of Aerospace Engineering
Georgia Institute of Technology

Dr. Magnus Egerstedt
School of Electrical and Computer Engineering
Georgia Institute of Technology

Date Approved: December 5^{th}, 2016

TABLE OF CONTENTS

LIST OF TABLES . . . . . **v**

LIST OF FIGURES . . . . . **vi**

SUMMARY . . . . . **vii**

I INTRODUCTION **1**

1.1 Synchronized Spacecraft Attitude Control 1

1.2 Why Control Underactuated Spacecraft Clusters? 2

1.3 Objectives of this Thesis 4

1.3.1 Problem 1 4

1.3.2 Problem 2 5

1.3.3 Extension of Problem 1 6

1.4 Thesis Outline 6

II PRELIMINARY MATERIAL **7**

2.1 Introduction 7

2.2 Notation 7

2.3 Spacecraft Model 8

2.4 A Graph Theoretic Representation of the Spacecraft Communication Topology 9

2.4.1 A Short Introduction 9

2.4.2 Notation of the Communication Graph 10

2.4.3 A Few Useful Graph Theoretic Tools 11

2.5 The Attitude Parameterization 15

2.5.1 A Short Introduction 15

2.5.2 Defining the w-z Parameters 16

2.5.3 The Kinematics of the w-z parameters 18

III PARTIAL ATTITUDE SYNCHRONIZATION BETWEEN UNDERACTUATED SPACECRAFT TOWARDS A FIXED INERTIAL DIRECTION **20**

3.1 Introduction 20

3.2 Problem Definition 20

3.3 Main Result for Solving Problem 1 21

3.4 Simulation 1: 4-Spacecraft Network With Inertial Velocity Feedback . . . 25

IV PARTIAL ATTITUDE SYNCHRONIZATION BETWEEN UNDERACTUATED SPACECRAFT USING RELATIVE VELOCITY FEEDBACK 29

4.1 Introduction . . . 29

4.2 Problem Definition . . . 29

4.3 Main Result for Solving Problem 2 . . . 30

4.3.1 Simulation 2: 4-Spacecraft Network With Relative Velocity Feedback 34

V PARTIAL ATTITUDE SYNCHRONIZATION BETWEEN UNDERACTUATED SPACECRAFT TOWARDS A SPECIFIED FIXED INERTIAL DIRECTION . . . 38

5.1 Introduction and Problem Definition . . . 38

5.2 Main Result for Solving the Extension of Problem 1 . . . 38

5.2.1 Simulation 3: Leader-Follower Extension to Proposition 1 . . . 40

VI CONCLUSION . . . 44

6.1 Summary . . . 44

6.2 Future Work . . . 44

REFERENCES . . . 46

LIST OF TABLES

1 Common notation used throughout this thesis 7

LIST OF FIGURES

1 An arborescence with its vertices and edges labeled. 11

2 An arborescense with its vertices and edges labeled. 13

3 Visualization of the stereographic projection of $\hat{\mathbf{b}}_3^j$ in the $\hat{\mathbf{b}}^i$ frame. 17

4 Example communication graph with undirected edges. 24

5 Example communication graph with relabeled nodes and directed edges. . . 24

6 The w parameter state histories for Problem 1: (a) w parameters of Spacecraft 2 in the frame of Spacecraft 1; (b) w parameters of Spacecraft 1 in the frame of Spacecraft 3; (c) w parameters of Spacecraft 2 in the frame of Spacecraft 3; (d) w parameters of Spacecraft 4 in the frame of Spacecraft 3. 27

7 Snapshots at different phases of the simulation for Problem 1. 28

8 The w parameter state histories for Problem 2: (a) w parameters of spacecraft 2 in the frame of spacecraft 1; (b) w parameters of spacecraft 1 in the frame of spacecraft 3; (c) w parameters of spacecraft 2 in the frame of spacecraft 3; (d) w parameters of spacecraft 4 in the frame of spacecraft 3. 36

9 Snapshots at different phases of the simulation for Problem 2. 37

10 The w parameter state histories for the extension to Problem 1: (a) w parameters of spacecraft 2 in the frame of spacecraft 1; (b) w parameters of spacecraft 1 in the frame of spacecraft 3; (c) w parameters of spacecraft 2 in the frame of spacecraft 3; (d) w parameters of spacecraft 4 in the frame of spacecraft 3. 42

11 Snapshots at different phases of the simulation for the extension to Problem 1. 43

SUMMARY

Numerous works have investigated problems concerning the complete attitude consensus of multi-spacecraft systems as well as the attitude control of an underactuated spacecraft, where only two or fewer control torques are available. There have been, however, no works which have focused on the attitude consensus problem among multiple *underactuated* spacecraft successfully, to the author's knowledge. In this thesis, three control laws are presented to solve three problems concerning this rather underdeveloped area. In the first problem, the aim is to achieve partial attitude consensus amongst a network of underactuated spacecraft in which the uncontrolled axis of each spacecraft points in the same fixed inertial direction. In the second problem, the aim is to solve a similar system, where the pointing direction of the uncontrolled axes is no longer constrained to point along a fixed direction and instead may rotate in inertial space. The third problem is an extension of the first problem where the leaderless system is expanded to that of a leader-follower type so that the intended final pointing direction of the uncontrolled axes of the spacecraft may be specified. Utilizing a novel attitude parameterization, the control laws are able to take the form of a linear controller for the first problem, its extension, and for the second problem if the spacecraft are axisymmetric. As a result of the three control laws, the desired partial attitude consensus state becomes almost globally asymptotically stable.

CHAPTER I

INTRODUCTION

1.1 Synchronized Spacecraft Attitude Control

Distributed control of multi-agent systems has gained an increase in attention over the past two decades. In comparison to a single agent, utilizing multiple agents features many advantages that otherwise can be difficult to include in a design, such as increased feasibility, robustness, fault tolerance, or expandability, to name a few [14]. The importance of these advantages also rises as the environment becomes more hostile or inaccessible, or the objective becomes more complex; such is the case especially when space operations are considered. It is therefore of no surprise that multi-agent control and synchronization of spacecraft has received much attention within the controls community.

In terms of spacecraft attitude synchronization, the majority of the literature up until now has assumed that complete control of the spacecraft is available. This area has seen a healthy progression of results and several results using a variety of different approaches have been proposed over the years to solve this problem [34, 6, 13, 17, 32, 7, 18, 21, 9, 8, 20, 3, 2, 1].

For instance, in [34, 6] the utilization of a leader-follower approach was used for solving problems related to formation flying. Formation control laws for maintaining attitude alignment was also presented in [13] by requiring that spacecraft communication be restricted to a simple ring structure. The problem of spacecraft attitude stabilization in a network where each spacecraft may spin about its unstable axis was solved in [17]. Attitude tracking control laws which globally asymptotically stabilize the attitude of the spacecraft within a formation was developed and analyzed in [32]. The stabilization of rigid bodies so that their orientations and angular velocity vectors align was shown using a graph theoretic approach in [7]. The synchronization of both the translation and rotation of rigid body networks was addressed in [18]. Extensions using energy shaping methods were provided in [21]. Multiple robust controllers which achieved attitude coordinated control of a spacecraft formation was

proven in [9]. Some works have also expanded on the cooperative attitude control to handle scenarios where only a subset of the spacecraft have knowlege of an attitude reference [8, 20]. Other results propose control laws that omit the need for an inertial reference [3], control laws that omit the need for angular velocity measurements [2, 20], and control laws that incorporate communication delays [9, 1].

In contrast to these references, attitude control of a single spacecraft has also been explored for the scenario in which complete attitude control is unavailable. Publications such as [27, 12, 25, 5, 26, 30, 31, 33, 22] have focused on the underactuated spacecraft control problem, where torques about only two axes are available, addressing not only the theoretical limitations of this problem, but also the practical utility for spacecraft which have experienced irreversible failures. For example, [12] showed that if the total angular momentum of a spacecraft is zero, then a discontinuous feedback control strategy can be used to stabilize any equilibrium attitude in finite time. The reference [26] provides a good review concerning spacecraft control results after an actuator failure. References [30, 33] consider spacecraft attitude control with bounded inputs and periodical oscillation disturbances, respectively. Finally, [30] provides a more applied result for underactuated control where stabilizing and tracking feeback control laws subject to input constraints were demonstrated.

Upon the subject of combining the above notions, no results thus far exist which focus on the coordinated control of networks of underactuated spacecraft successfully, to the author's knowledge. It is the idea of multi-spacecraft consensus control in which this thesis will attempt to achieve.

1.2 Why Control Underactuated Spacecraft Clusters?

Many publications concerning consensus control of spacecraft have been published, so why is underactuated and partial consensus control worth investigating? Aside from the theoretical excitement and challenges this problem offers, there are direct practical benefits as well.

On a theoretical note, controlling a subset of the dynamics of individual agents which react to each other in order to drive the system as a whole into as state of partial agreement

is a complex and seemingly cumbersome problem in itself. The dependencies of a networked multi-spacecraft system's overall behavior include the motion of individual agents, which is governed by coupled nonlinear equations, and the communication links between these agents. Additional requirements can be placed such as switching communication topologies (perhaps due to state-dependent communication channels), communication lag, more complex objectives such as solving a coverage problem or achieving a cooperative goal, the introduction of noise, etc., and so a wealth of different avenues exist that lend themselves towards extending underactuated cooperative control well beyond the scope of work achieved here.

On a more practical side, controlling an underactuated spacecraft cluster implies knowing how one could still utilize a spacecraft formation in the event of actuator or sensor failures, an ability that further extends the robustness inherent in a distributed formation. This also provides additional options during spacecraft mission design phases. One immediate example of this possibly is when considering a fractionated spacecraft. The idea of a fractionated spacecraft is to utilize a collection of smaller spacecraft operating in tight formation as opposed to a single large spacecraft in the hopes that utilizing several smaller, simpler spacecraft for a mission would prove more benficial and cheaper than a single monolithic complex one [15, 19]. Often, sensors where only the pointing of the boresight is necessary (such as optical spectrometers or high-gain communication antennas) are used, and so in a fractionated spacecraft, individual spacecraft containing only these sensors may be designed omitting control about the boresignt axis. Another example is when utilizing a collection of spacecraft to observe a distant star using boresignt sensors or to maintain communication capabilities when a subset of the spacecraft may have their field of view or communication path blocked. All spacecraft would capably match their pointing with each other no matter which spacecraft know their pointing objective. In adition to these, another example is when operating multiple small spacecraft which feature only electromagnetic actuation. Because of the nature of this type of actuation, there is always a single axis which is not directly controllable and has a direction dependent upon the spacecraft's location in orbit [24, 36]. In this scenario, without the addition of thrusters or reaction wheels or

some other form of actuation, each spacecraft is inherently underactuated. It is unclear how multiple underactuated spacecraft will influence each other when the underactuated axis is changing in time or when this axis is different for each spacecraft, but in desiring to keep costs low for multi-spacecraft missions, the question of how to control a cluster of spacecraft with only magnetorquer-based attitude control is an important one.

In considering missions such as these, each spacecraft may also have their control about the sensory/antenna boresignt axis omitted or halted, or additional control methods excluded. In these examples, the ability to reduce the costs and complexity of the system are of potential gain, and as will be shown, the pointing requirements necessary can be achievable even with the inclusion of spacecraft dynamics.

1.3 Objectives of this Thesis

One of the fundamental problems concerning the control of multi-agent systems is that of achieving some sort of consensus. Solving the consensus problem provides the underlying foundation for a number of problems or extensions, from maintaining a certain temperature reading agreement from multiple sensors in a furnace, a flow rate amongst multiple valves, the rendezvous of aircraft at a specified location, or the attitude alignment of sensors on a spacecraft. It is therefore the focus of this thesis with regards to attitude alignment to ultimately control a network of communicating underactuated spacecraft. Specifically, the main objective is to manipulate, in a distributed fashion, the system of spacecraft so that they converge towards a partial consensus such that the uncontrolled axis of each spacecraft may point towards the same direction in inertial space. Finding the solution of two problems, denoted as Problem 1 and Problem 2, and an extension associated with this objective comprise the majority of this research effort.

1.3.1 Problem 1

The first problem considered in this thesis deals with finding a solution to a simple partial attitude alignment problem. The agents that make up the system we wish to control are underactuated spacecraft, that is, torque control is unavailable about all three principal axes. With the available control, the objective is to develop a distributed control law

capable of partially synchronizing this group of underactuated spacecraft where the final pointing direction of all uncontrolled axes is the same and fixed in inertial space.

Problem 1 proposes to provide the groundwork necessary to enable a spacecraft cluster to perform missions that are cheaper and more robust than what is currently possible. The resulting control law may allow the design of spacecraft in which actuators such as a momentum wheel or thruster pair can be omitted, used in a minimal fashion, or allowed to fail in a cluster without compromising mission objectives. The types of missions in which exploring Problem 1 will be beneficial include those in which the directional pointing of an axis is the primary objective such as the communication through high gain antenna or data collection via sensor boresignts (i.e., optical spectrometer, telescope) over sufficiently long ranges.

1.3.2 Problem 2

The second problem considered is similar Problem 1; it deals with finding a solution to the partial attitude alignment problem. It differs from Problem 1 in that the control inputs are given a restriction: they can only rely on relative information; but this restriction generalizes the problem somewhat in that since there is no explicit feedback in the control due to inertial information, the final consensus state may be free to rotate in the inertial frame. The objective of Problem 2 is then to develop a distributed control law capable of partially synchronizing a group of underactuated spacecraft where the final pointing direction of all uncontrolled axes is the same and as mentioned, but not necessarily fixed in inertial space.

The efforts in Problem 2 provide similar benefits as those from Problem 1 with a more general application. For example, the use of multiple underactuated spacecraft in orbit together to survey a geographic location or to communicate via a high gain antenna to another passing spacecraft could be plausible. In addition, since the control law relies only upon relative state information, it may be possible to avoid the exchange of state information altogether and allow each spacecraft to obtain this relative information from its neighboring spacecraft independently through, for example, cameras.

1.3.3 Extension of Problem 1

In most practical scenarios, the pointing of a sensor towards a particular known direction is necessary such as when taking optical observations or communicating over a vast range. Therefore, a natural extension to achieving a general consensus is the incorporation of a leader to follow. This leader-follower scenario may be applied to Problem 1, and so the purpose of this extension is to show that if a single spacecraft in a group of underactuated spacecraft is provided a reference fixed in inertial space, then the final pointing direction of all uncontrolled axes points towards this reference.

1.4 Thesis Outline

The remainder of this thesis is broken into five chapters. Chapter 2 introduces the preliminary material necessary in understanding the specific tools used in the problems and their analyses. Chapter 3, 4, and 5 are dedicated to the introduction of and solutions to Problem 1, Problem 2, and the Extension of Problem 1, respectively, with each containing, in addition, the analytical proof and simulation results that demonstrate the abilities of the found corresponding control laws. Chapter 6 concludes the efforts of this thesis and mentions some foreseeable possibilities for future work.

CHAPTER II

PRELIMINARY MATERIAL

2.1 Introduction

In tackling the problems mentioned, there are a number of items one must first become familiar with. This chapter is dedicated towards explaining those necessary items. In particular, the mathematical notation and concepts used throughout this document concerning the spacecraft considered are introduced. These include their communication, the parameterization used for describing spacecraft orientation, and their associated specific results used later on. This chapter is organized in the following way. First, much of the mathematical notation used in the subsequent sections is introduced. Next follows the dynamical model used to illustrate the spacecraft motion in consideration. The framework relied upon in depicting the communication architecture present amongst the spacecraft is presented in terms of tools taken from graph theory. Finally, what is known as the w-z attitude parameterization is described as an ideal representation of an underactuated spacecraft's attitude for the problems considered.

2.2 Notation

Table 1: Common notation used throughout this thesis

i	$\triangleq$	index referring to a specific spacecraft.
$\hat{\mathbf{b}}^i$	$\triangleq$	the body frame of spacecraft i with basis vectors $\hat{\mathbf{b}}_1^i$, $\hat{\mathbf{b}}_2^i$, and $\hat{\mathbf{b}}_3^i$
I^i	$\triangleq$	the principal inertia tensor of spacecraft i
ω^i	$\triangleq$	the inertial angular velocity of frame i described in frame i
$S(x)$	$\triangleq$	the skew symmetric matrix representing the cross product between two vectors: $S(x_1)x_2 = -\overrightarrow{x}_1 \times \overrightarrow{x}_2$
u^i	$\triangleq$	the control torque input to spacecraft i

$\mathcal{V}$	$\triangleq$	the set consisting of all spacecraft s_i forming the vertices v_i in the graph $\mathcal{G}$
$\mathcal{E}$	$\triangleq$	the set consisting of all edges in the graph $\mathcal{G}$
$\mathcal{N}_i$	$\triangleq$	the set of vertices that are in direct communication with vertex i
$\mathcal{G}$	$\triangleq$	the communication graph of a system of networked spacecraft
$\mathcal{D}(\mathcal{G})$	$\triangleq$	the incidence matrix for the graph $\mathcal{G}$
$\mathcal{L}(\mathcal{G})$	$\triangleq$	the Laplacian matrix for the graph $\mathcal{G}$
R_j^i	$\triangleq$	the rotation matrix that transforms elements from frame j to frame i
w^{ij}	$\triangleq$	the w parameters describing the $\hat{\mathbf{b}}_3^j$ in the frame of $\hat{\mathbf{b}}^i$
η^i	$\triangleq$	the partial inertial angular velocity of frame i described in frame i
$\delta\eta^{ij}$	$\triangleq$	the partial angular velocity descrepancy between frame frame i and frame j described in frame i
$\tilde{R}_j^i$	$\triangleq$	the upper left 2×2 sub block of R_j^i

2.3 Spacecraft Model

Although the focus in this chapter involves multiple spacecraft, each one is assumed to be represented in the same way. Each spacecraft is therefore modeled as a rigid body with control torque inputs entering the dynamics along the principal inertia axes. In this spirit, let any particular spacecraft under consideration be represented by the index i. The spacecraft i has associated with it a body-fixed frame $\hat{\mathbf{b}}^i = (\hat{\mathbf{b}}_1^i, \hat{\mathbf{b}}_2^i, \hat{\mathbf{b}}_3^i)$, where $\hat{\mathbf{b}}_1^i$ is the frame axis along the first principal axis of the spacecraft, $\hat{\mathbf{b}}_2^i$ is the frame axis along the second principal axis, and $\hat{\mathbf{b}}_3^i$ is the frame axis along the third principal axis. The notation $I^i = \mathrm{diag}(I_1^i, I_2^i, I_3^i)$, with inertias I_1^i, I_2^i, and I_3^i along the $\hat{\mathbf{b}}_1^i$, $\hat{\mathbf{b}}_2^i$, and $\hat{\mathbf{b}}_3^i$ axes, respectively, is taken to represent the principal inertia tensor for the spacecraft i while $\omega^i = [\omega_1^i, \omega_2^i, \omega_3^i]^\mathsf{T} \in \mathbb{R}^3$ is taken to represent the inertial angular velocity of spacecraft i

expressed in the $\hat{\mathbf{b}}^i$ frame. Each spacecraft is considered to be a rigid body and thus features the dynamics of rigid body motion. For a spacecraft i, the notation describing its dynamics are

$$I^i\dot{\omega}^i = S(\omega^i)I^i\omega^i + u^i, \tag{1}$$

where $S(\cdot)$ represents the skew symmetric matrix representing the cross product between two vectors, i.e., $S(x_1)x_2 = -\overrightarrow{x}_1 \times \overrightarrow{x}_2$, and $u^i = [u_1^i, u_2^i, u_3^i]^\mathsf{T} \in \mathbb{R}^3$ represents the control torque influencing the spacecraft.

Since the objective is to control only underactuated spacecraft with two control torques, without loss of generality, $u_3^i \equiv 0$ may be set and therefore allows the control inputs u_1^i and u_2^i to remain free for design. Thus, the complete dynamical model of each spacecraft i throughout the remainder of this work is

$$\begin{aligned} I_1^i\dot{\omega}_1^i &= (I_2^i - I_3^i)\omega_2^i\omega_3^i + u_1^i, \\ I_2^i\dot{\omega}_2^i &= (I_3^i - I_1^i)\omega_1^i\omega_3^i + u_2^i, \\ I_3^i\dot{\omega}_3^i &= (I_1^i - I_2^i)\omega_1^i\omega_2^i. \end{aligned} \tag{2}$$

2.4 A Graph Theoretic Representation of the Spacecraft Communication Topology

2.4.1 A Short Introduction

Synchronization of a multi-agent system, such as the spacecraft network we will be considering here, involves controlling the state of the agent through its dynamics, while incorporating some information concerning the states of the other agents in the network in order to drive the system to the desired consensus. This approach relies upon the local non-consensus state of the network, evaluated by the individual members, in order to drive the individual spacecraft in the cluster to a state 'closer' towards synchronization. Following the introduction of the dynamics assumed for each member of the network to control a member-specific state, this document now focuses on how the communication of state information is represented as well as the graph theoretic tools used in the analyses that incorporates the network's communication topology.

2.4.2 Notation of the Communication Graph

Let the network connectivity graph in consideration, denoted as $\mathcal{G}$, consist of a total of N vertices, or equivalently, N agents, and let the vertex set $\mathcal{V} = \{1, 2, \cdots, N\}$ be the set containing all vertices of the network so that a vertex in the network, labeled as i, is a member of $\mathcal{V}$, i.e. $i \in \mathcal{V}$. Suppose that there exists a second vertex $j \in \mathcal{V}$ that is in communication with vertex i, or more specifically, that information held by a vertex j may be observed by vertex i (for our purposes in this example, the information available for an agent i to observe is considered to be the state of agent j). Since information may travel from vertex j to vertex i, we say the edge (j, i) exists in the network. If the network contains a total of M edges, then the set of all edges in the network is defined as $\mathcal{E} = \{(j, i) \in \mathcal{V} \times \mathcal{V} \mid j \in \mathcal{N}_i\} = \{\varepsilon_1, \cdots, \varepsilon_M\}$, where $\mathcal{N}_i$ is a set of all vertices j in which an edge (j, i) exists. $\mathcal{N}_i$ is the *neighborhood* of vertex i.

A communication graph consisting of the vertices contained in $\mathcal{V}$ and the edges contained in $\mathcal{E}$ is denoted as $\mathcal{G}(\mathcal{V}, \mathcal{E})$. If $\mathcal{E}$ contains directed edges, then the graph $\mathcal{G}$ is said to be a directed graph. If every edge in $\mathcal{E}$ is such that $j \in \mathcal{N}_i$ if and only if $i \in \mathcal{N}_j$, for all $i, j \in \mathcal{V}$, $i \neq j$, the graph $\mathcal{G}$ is said to be an undirected graph. If the edges (j, i) and (i, j) exist between vertices $i, j \in \mathcal{V}$, then it is considered to be a single undirected edge and is simply denoted as (j, i) (while this simplification may cause some confusion, the distinction concerning whether the edge (j, i) is either directed or undirected will be provided).

Different types of graphs exist for different edge arrangements. If a graph is such that the edges are undirected and there is *exactly* one unique path between any two vertices, then the graph is acyclic and is called a *tree*. A tree graph contains $M = N - 1$ undirected edges (or $2M$ directed edges). If a directed graph is such that for a vertex $i \in \mathcal{V}$, there is exactly one directed path from i to every $j \in \mathcal{V} \setminus i$, it is called an *arborescence* and takes the form of a directed rooted tree with i as the root; as a consequence, all vertices which are not the root have at most one in-going edge. An example of a graph which takes the form of an arborescence is provided in Figure 1. If there exists some path (not necessarily bi-directional) between a vertex i and j in a graph, then those vertices are said to be connected. If every pair of vertices in a graph is connected, then the graph is a connected

graph.

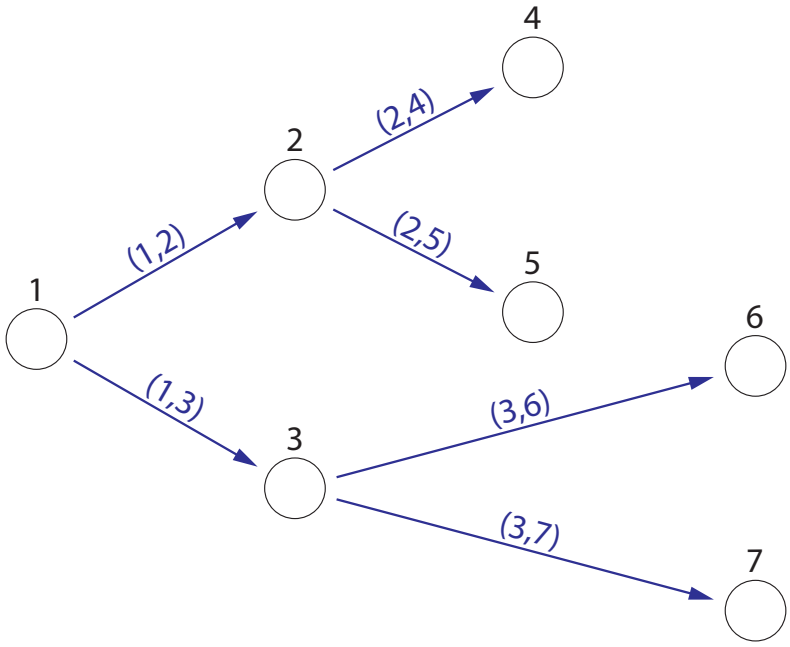

Figure 1: An arborescence with its vertices and edges labeled.

2.4.3 A Few Useful Graph Theoretic Tools

A few tools present in graph theory prove themselves to be very useful in the analysis of multi-agent systems. One of these tools is the graph incidence matrix defined below.

Definition 1. *Given a directed graph $\mathcal{G}$, the incidence matrix, denoted by $\mathcal{D}(\mathcal{G}) \in \mathbb{R}^{N\times M}$, is defined as*

$$[\mathcal{D}(\mathcal{G})]_{ie} = \begin{cases} 1, & \text{if } (j,i) = \varepsilon_e \in \mathcal{E}, \\ -1, & \text{if } (i,j) = \varepsilon_e \in \mathcal{E}, \\ 0, & \text{otherwise.} \end{cases} \tag{3}$$

The incidence matrix $\mathcal{D}(\mathcal{G})$ for an undirected graph is taken to be the same as for a directed graph where for each edge in the undirected graph, a direction is arbitrarily chosen. Notice that each column of $\mathcal{D}(\mathcal{G})$ sums to 0 and contains a 1 (in-going) and a -1 (out-going) for each end of the corresponding edge. A property of incidence matrices is that for a tree graph, $\mathcal{D}(\mathcal{G})$ is full column rank.

Let $\mathcal{D}^+(\mathcal{G})$ denote the pseudo-inverse of $\mathcal{D}(\mathcal{G})$. Then for a connected graph $\mathcal{G}$, it follows that

$$\mathrm{I}_N - \mathcal{D}(\mathcal{G})\mathcal{D}^+(\mathcal{G}) = \frac{1}{N}\mathbf{1}_{N\times N}, \tag{4}$$

where $\mathbf{1}_{N\times N}$ represents the $N \times N$ matrix consisting of all ones [4].

Another tool often used in graph theory is the graph Laplacian which represents the connectivity structure between each of the nodes in the form of a matrix.

Definition 2. *The Laplacian matrix for a graph $\mathcal{G}$, denoted by $\mathcal{L}(\mathcal{G}) \in \mathbb{R}^{N\times N}$, is defined as*

$$[\mathcal{L}(\mathcal{G})]_{i,j} = \begin{cases} \deg_{\text{in}}(i), & \text{if } i = j, \\ -1, & \text{if } (j,i) \in \mathcal{E}, \\ 0, & \text{otherwise}, \end{cases} \tag{5}$$

where $\deg_{\text{in}}(i)$ is the in-degree of vertex i.

For undirected graphs, the matrix $\mathcal{L}(\mathcal{G})$ is positive semidefinite. If $\mathcal{G}$ is connected, then $\mathcal{L}(\mathcal{G})$ contains a single eigenvalue at 0 and the corresponding eigenvector is a multiple of the vector of ones $\mathbf{1}_N = [1, \cdots, 1]^\mathsf{T} \in \mathbb{R}^N$.

The next few results are necessary for the specific problems considered here, and so they are presented as Lemmas. The following is a well known fact in graph theory [10].

Lemma 1. *Consider an arborescence $\mathcal{G}$ having N vertices and $M = N - 1$ edges and incidence matrix $\mathcal{D}(\mathcal{G}) \in \mathbb{R}^{N\times M}$. Let $\mathcal{D}_r(\mathcal{G}) \in \mathbb{R}^{M\times M}$ be the resulting matrix achieved from $\mathcal{D}(\mathcal{G})$ after deleting its r^{th} row. An ordering of vertices and edges always exists such that $\mathcal{D}_r(\mathcal{G})$ is upper triangular.*

Proof. Begin labeling the vertices of the arborescence by increasing index from the root. One way this can be achieved is by labeling the vertices' indices sequentially by their walk from the root in the following way: assign the index 1 to the root of the arborescense, then continue the sequential labeling of all vertices that are a walk 1 from the root, then walk 2 from the root, and so on. Since each vertex in the graph excluding the root has a single in-going edge, assign the in-going edge ε_e to the vertex $i > 1$ the index $e = i - 1$. From this

labeling scheme, it follows that since for every edge $\varepsilon_e = (j, i)$, where $i = e + 1$ and $j \leq e$, it follows directly from (3) that $\mathcal{D}_r(\mathcal{G})$ is upper triangular. $\square$

Different labeling schemes may be used to construct $\mathcal{D}_r(\mathcal{G})$ such that it is lower triangular as well. This follows from the fact that any upper triangular matrix may be permuted to form a lower triangular matrix and that a permutation of any two rows or columns in an incidence matrix corresponds to a relabeling of the vertices or edges of the graph, respectively. An example of executing Lemma 1 is provided with the graph labeling given in Figure 2 and the resulting incidence matrices given in (6). Note that while in this example r is taken to be the root vertex, it does not necessarily have to be, and a simple reordering of the vertices is sufficient to produce again a $\mathcal{D}_r(\mathcal{G})$ which is triangular.

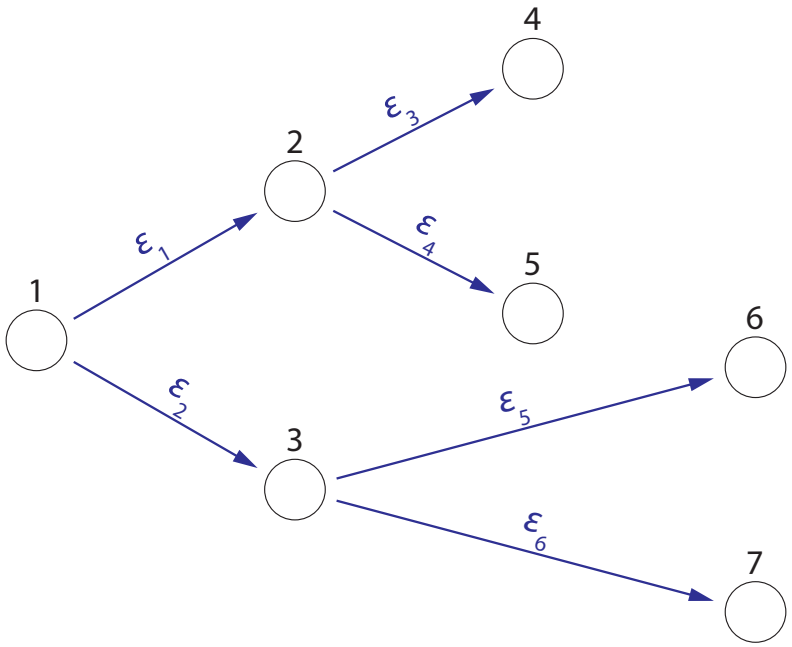

Figure 2: An arborescense with its vertices and edges labeled.

$$\mathcal{D}(\mathcal{G}) = \begin{bmatrix} -1 & -1 & 0 & 0 & 0 & 0 \\ 1 & 0 & -1 & -1 & 0 & 0 \\ 0 & 1 & 0 & 0 & -1 & -1 \\ 0 & 0 & 1 & 0 & 0 & 0 \\ 0 & 0 & 0 & 1 & 0 & 0 \\ 0 & 0 & 0 & 0 & 1 & 0 \\ 0 & 0 & 0 & 0 & 0 & 1 \end{bmatrix} \quad \Rightarrow \quad \mathcal{D}_1(\mathcal{G}) = \begin{bmatrix} 1 & 0 & -1 & -1 & 0 & 0 \\ 0 & 1 & 0 & 0 & -1 & -1 \\ 0 & 0 & 1 & 0 & 0 & 0 \\ 0 & 0 & 0 & 1 & 0 & 0 \\ 0 & 0 & 0 & 0 & 1 & 0 \\ 0 & 0 & 0 & 0 & 0 & 1 \end{bmatrix} \tag{6}$$

This next lemma is a rather new extension of Lemma 1.

Lemma 2. *Consider an undirected tree $\mathcal{G}$ having N vertices and $M = N - 1$ edges and incidence matrix $\mathcal{D}(\mathcal{G}) \in \mathbb{R}^{N \times M}$. Let the matrix $\tilde{\mathcal{D}}(\mathcal{G}) \in \mathbb{R}^{rN \times sM}$ be such that it has the same structure as $\mathcal{D}(\mathcal{G}) \otimes A$, where $A \in \mathbb{R}^{r \times s}, r \geq s$, constructed as follows. For every element in $\mathcal{D}(\mathcal{G})$, there corresponds an $r \times s$ submatrix in $\tilde{\mathcal{D}}(\mathcal{G})$ such that $\tilde{\mathcal{D}}(\mathcal{G})$ is given by*

$$[\tilde{\mathcal{D}}(\mathcal{G})]_{\alpha,\beta} = \begin{cases} \Phi_{ie} & \text{if } (j,i) = \varepsilon_e \in \mathcal{E}, \\ \Psi_{ie} & \text{if } (i,j) = \varepsilon_e \in \mathcal{E}, \\ 0 & \text{otherwise}, \end{cases} \tag{7}$$

where α and β indicate a range of indices for the submatrix $[\tilde{\mathcal{D}}(\mathcal{G})]_{\alpha,\beta}$ where $r(i-1)+1 \leq \alpha \leq ri$ and $s(e-1)+1 \leq \beta \leq se$, and where $\Phi_{ie}, \Psi_{ie} \in \mathbb{R}^{r \times s}$. Then, if either Φ_{ie} or Ψ_{ie} is full column rank for all $i = 1, \ldots, N$ and $e = 1, \ldots, M$, then an edge orientation exists such that $\tilde{\mathcal{D}}(\mathcal{G})$ is also full column rank.

Proof. Notice that since $\mathcal{G}$ is a tree, $\mathcal{D}(\mathcal{G})$ is full column rank. Furthermore, by Lemma 1, an ordering of vertices and edges always exists such that the upper $(N-1) \times M$ submatrix of $\mathcal{D}(\mathcal{G})$ is lower triangular. Since $\mathcal{D}(\mathcal{G})$ may be constructed for an undirected graph through arbitrarily directing each link, then without loss of generality, we choose Φ_{ie}, for all $i = 1, \ldots, N$ and $e = 1, \ldots, M$, to be full column rank in which case Ψ_{ie} need not be full column rank for any $i = 1, \ldots, N$ and $e = 1, \ldots, M$. The matrix $\tilde{\mathcal{D}}(\mathcal{G})$ may be constructed such that the upper $r(N-1) \times sM$ submatrix is lower block triangular where the blocks along

the diagonal are the appropriate matrices Φ_{ie}. It follows directly that $\tilde{\mathcal{D}}(\mathcal{G})$ is full column rank. □

It is possible to further generalize Lemma 2 such that the matrices Φ_{ie} and Ψ_{ie} may be of different row and column sizes depending on the vertex and the edge indices, respectively, but this is unnecessary for the problems presented in this thesis.

2.5 The Attitude Parameterization

2.5.1 A Short Introduction

Analyzing the partial relative states of a system with coupled dynamics can impose some challenges with one being how to best describe the state itself. The problems considered here concern an underactuated system where the states whose dynamics are directly affected by the control input as well as the states of interest for consensus may be considered in some sense the same objects. Thus, an advantageous scenario would be to describe the state of the system in such a way that the states which we care about are somewhat "separated" from those states which are of minimal interest. For this reason, a unique attitude parameterization is chosen.

The w-z attitude parameterization, introduced by Tsiotras and Longuski in [28, 29], provides a formulation of the attitude of a spacecraft so that a single axis may be defined without the inclusion of the spacecraft's orientation about that axis. For our application, where a partial consensus is sought in terms of aligning a single body axis of many spacecraft by controlling the torque about each of the two adjacent axes, the w-z parameterization is an extremely appropriate descriptor. The w parameters arise upon taking the axis of interest and stereographically projecting it onto a plane where a two-dimensional vector is formed which is represented here as the parameters themselves. In terms of two relative frames $\hat{\mathbf{b}}^1$ and $\hat{\mathbf{b}}^2$ and letting the stereographic plane be formed from the first two axes of frame $\hat{\mathbf{b}}^1$, the w parameters formed from the projection of the third axis of frame $\hat{\mathbf{b}}^2$ are directly related to the minimal amount of rotation through the first two axes of frame $\hat{\mathbf{b}}^1$ necessary to remove any non-zero angle between the two third axes of both frames. This point will be elaborated on more as the parameters are formally introduced.

2.5.2 Defining the w-z Parameters

The w-z attitude parameterization is a way to describe the attitude discrepancy between two reference frames which henceforth will be represented by the body-fixed frames $\hat{\mathbf{b}}^i$ and $\hat{\mathbf{b}}^j$ for spacecraft i and j, respectively. The rotation matrix that transforms vectors from frame $\hat{\mathbf{b}}^j$ to frame $\hat{\mathbf{b}}^i$ will be denoted by R^i_j and can be decomposed into two successive rotations according to the two parameters w^{ij} and z^{ij} as follows [28, 29].

$$R^i_j(\mathrm{w}^{ij}, z^{ij}) = R^i_{j'}(\mathrm{w}^{ij}) R^{j'}_j(z^{ij}), \tag{8}$$

where j' represents the intermediate frame $\hat{\mathbf{b}}^{j'}$ after the first rotation by z^{ij}. The matrix $R^{j'}_j(z^{ij})$ is the initial rotation about the $\hat{\mathbf{b}}^j_3$ axis in the positive direction by an angle z^{ij}, resulting in the intermediate frame $\hat{\mathbf{b}}^{j'}$. It is therefore given by

$$R^{j'}_j(z^{ij}) = \begin{bmatrix} \cos(z^{ij}) & \sin(z^{ij}) & 0 \\ -\sin(z^{ij}) & \cos(z^{ij}) & 0 \\ 0 & 0 & 1 \end{bmatrix}. \tag{9}$$

From this intermediate frame, we desire the third axis of the frame $\hat{\mathbf{b}}^j$ (also the third axis of the intermediate frame) to be described with respect to the final body frame $\hat{\mathbf{b}}^i$. This is accomplished by describing the $\hat{\mathbf{b}}^j_3$ vector in the $\hat{\mathbf{b}}^i$ frame as $\hat{\mathbf{b}}^j_3 = \hat{\mathbf{b}}^{j'}_3 = a^{ij}\hat{\mathbf{b}}^i_1 + b^{ij}\hat{\mathbf{b}}^i_2 + c^{ij}\hat{\mathbf{b}}^i_3$. This vector is then stereographically projected onto the $\hat{\mathbf{b}}^i_1$-$\hat{\mathbf{b}}^i_2$ plane to obtain a new vector with components w^{ij}_1 and w^{ij}_2, defined below

$$\mathrm{w}^{ij}_1 = \frac{b^{ij}}{1 + c^{ij}}, \qquad \mathrm{w}^{ij}_2 = \frac{-a^{ij}}{1 + c^{ij}}. \tag{10}$$

The parameters w^{ij}_1 and w^{ij}_2 can be used to describe how far to rotate or "tilt" the $\hat{\mathbf{b}}^i_3$ axis away from the $\hat{\mathbf{b}}^j_3$ axis about the vector $\hat{\mathbf{h}} = \hat{\mathbf{b}}^j_3 \times \hat{\mathbf{b}}^i_3$ as depicted in Fig. 3. The rotation matrix $R^i_{j'}(\mathrm{w}^{ij})$ in (8), where $\mathrm{w}^{ij} = [\mathrm{w}^{ij}_1, \mathrm{w}^{ij}_2]^\mathsf{T} \in \mathbb{R}^2$, then describes the rotation about the unit vector $\hat{\mathbf{h}}$, and is given by [28]

$$R^i_{j'}(\mathrm{w}^{ij}) = \frac{1}{1 + \|\mathrm{w}^{ij}\|^2} \begin{bmatrix} 1 + (\mathrm{w}^{ij}_1)^2 - (\mathrm{w}^{ij}_2)^2 & 2\mathrm{w}^{ij}_1\mathrm{w}^{ij}_2 & -2\mathrm{w}^{ij}_2 \\ 2\mathrm{w}^{ij}_1\mathrm{w}^{ij}_2 & 1 - (\mathrm{w}^{ij}_1)^2 + (\mathrm{w}^{ij}_2)^2 & 2\mathrm{w}^{ij}_1 \\ 2\mathrm{w}^{ij}_2 & -2\mathrm{w}^{ij}_1 & 1 - \|\mathrm{w}^{ij}\|^2 \end{bmatrix}. \tag{11}$$

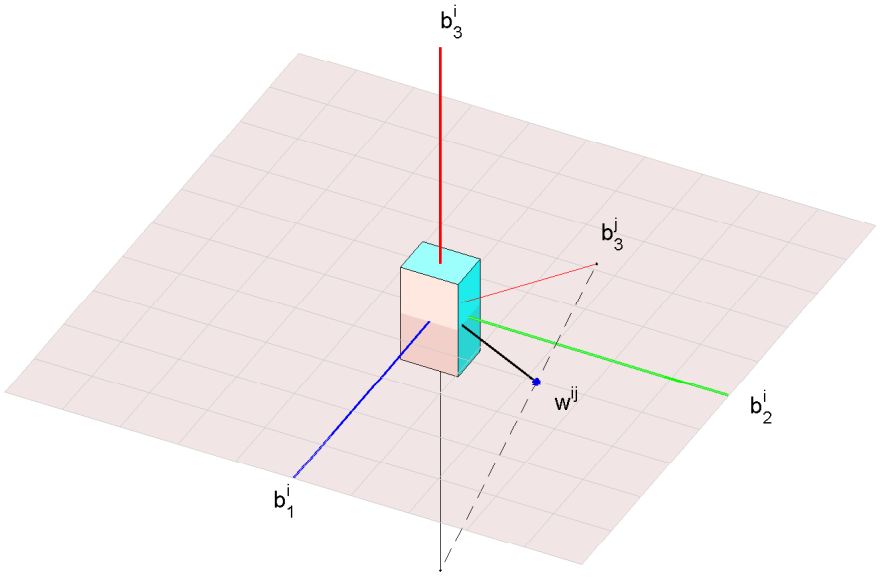

Figure 3: Visualization of the stereographic projection of $\hat{\mathbf{b}}_3^j$ in the $\hat{\mathbf{b}}^i$ frame.

As shown in Fig. 3, the w parameter offers a measure of the $\hat{\mathbf{b}}_3^j$ axis displacement from the $\hat{\mathbf{b}}_3^i$ axis in the form of a stereographic projection. Specifically, when the $\hat{\mathbf{b}}_3^j$ and $\hat{\mathbf{b}}_3^i$ axes are aligned, we have that $\mathrm{w}_1^{ij} = \mathrm{w}_2^{ij} = 0$. The angle θ^{ij} between the unit vectors $\hat{\mathbf{b}}_3^j$ and $\hat{\mathbf{b}}_3^i$ can be easily computed from w as

$$\theta^{ij} = \arccos\left(\frac{1 - (\mathrm{w}_1^{ij})^2 - (\mathrm{w}_2^{ij})^2}{1 + (\mathrm{w}_1^{ij})^2 + (\mathrm{w}_2^{ij})^2}\right). \tag{12}$$

Clearly, $\theta^{ij} = 0$ if and only if $\mathrm{w}_1^{ij} = \mathrm{w}_2^{ij} = 0$.

The following result provides a relation of two sets of the parameters, where each describes the frame the other is defined in.

Lemma 3. *Let $\hat{\mathbf{b}}^i$ and $\hat{\mathbf{b}}^j$ denote the two body reference frames for spacecraft i and j, respectively. In addition, let $\tilde{\mathrm{w}}^{ij} = [\mathrm{w}_1^{ij}, \mathrm{w}_2^{ij}, 0]^\mathsf{T} \in \mathbb{R}^3$, let $\tilde{\mathrm{w}}^{ji} = [\mathrm{w}_1^{ji}, \mathrm{w}_2^{ji}, 0]^\mathsf{T} \in \mathbb{R}^3$, and let $\tilde{R}_j^i \in \mathbb{R}^{2\times 2}$ represent the upper left 2×2 submatrix of R_j^i. Then*

$$\tilde{\mathrm{w}}^{ij} = -R_j^i \tilde{\mathrm{w}}^{ji} \tag{13}$$

and thus

$$\mathrm{w}^{ij} = -\tilde{R}^i_j \mathrm{w}^{ji} \tag{14}$$

and

$$(\mathrm{w}^{ij})^{\mathsf{T}} \mathrm{w}^{ij} = (\mathrm{w}^{ji})^{\mathsf{T}} \mathrm{w}^{ji}. \tag{15}$$

Proof. The rotation matrix that transforms vectors from frame $\hat{\mathbf{b}}^j$ to frame $\hat{\mathbf{b}}^i$ is R^i_j and depends on the values of w^{ij} and z^{ij} as follows

$$R^i_j = R^i_{j'}(\mathrm{w}^{ij}) R^{j'}_j(z^{ij}), \tag{16}$$

where $R^i_{j'}(\mathrm{w}^{ij})$ and $R^{j'}_j(z^{ij})$ as in (8) and similarly for $R^j_i = R^j_{i'}(\mathrm{w}^{ji}) R^{i'}_i(z^{ji})$. Using the fact that $R^i_j = [R^j_i]^{\mathsf{T}}$, the following two identities result immediately

$$\begin{aligned} -\mathrm{w}^{ji}_1 &= \mathrm{w}^{ij}_1 \cos(z^{ij}) - \mathrm{w}^{ij}_2 \sin(z^{ij}), \\ -\mathrm{w}^{ji}_2 &= \mathrm{w}^{ij}_1 \sin(z^{ij}) + \mathrm{w}^{ij}_2 \cos(z^{ij}). \end{aligned} \tag{17}$$

By substituting equations (17) and the rotation matrix expression in equation (16) into equation (13) proves the desired result. □

2.5.3 The Kinematics of the w-z parameters

Next, consider the kinematics of the w parameters. To this end, let the angular velocity of the $\hat{\mathbf{b}}^i$ frame with respect to the $\hat{\mathbf{b}}^j$ frame, expressed in the $\hat{\mathbf{b}}^i$ frame, be denoted as $\overrightarrow{\omega}^{ij} = \omega^{ij}_1 \hat{\mathbf{b}}^i_1 + \omega^{ij}_2 \hat{\mathbf{b}}^i_2 + \omega^{ij}_3 \hat{\mathbf{b}}^i_3$. Letting $\omega^i = [\omega^i_1, \omega^i_2, \omega^i_3]^{\mathsf{T}} \in \mathbb{R}^3$ represent the angular velocity of the $\hat{\mathbf{b}}^i$ frame with respect to the inertial frame, expressed in the $\hat{\mathbf{b}}^i$ frame, and define similarly ω^j, the components of $\overrightarrow{\omega}^{ij}$ are found by

$$\omega^{ij} = \omega^i - R^i_j \omega^j, \tag{18}$$

where $\omega^{ij} = [\omega^{ij}_1, \omega^{ij}_2, \omega^{ij}_3]^{\mathsf{T}} \in \mathbb{R}^3$. Taking the derivative of the $\hat{\mathbf{b}}^j_3$ unit vector expressed in the $\hat{\mathbf{b}}^i$ frame, yields [23, 11, 35]

$$\begin{bmatrix} \dot{a}^{ij} \\ \dot{b}^{ij} \\ \dot{c}^{ij} \end{bmatrix} = \begin{bmatrix} 0 & \omega^{ij}_3 & -\omega^{ij}_2 \\ -\omega^{ij}_3 & 0 & \omega^{ij}_1 \\ \omega^{ij}_2 & -\omega^{ij}_1 & 0 \end{bmatrix} \begin{bmatrix} a^{ij} \\ b^{ij} \\ c^{ij} \end{bmatrix}. \tag{19}$$

Using equations (10) and (19), the differential equations for the parameters w_1^{ij} and w_2^{ij} can be calculated as

$$\begin{aligned}\begin{bmatrix}\dot{\mathrm{w}}_1^{ij}\\ \dot{\mathrm{w}}_2^{ij}\end{bmatrix} &= \frac{1+(\mathrm{w}_1^{ij})^2+(\mathrm{w}_2^{ij})^2}{2}[\breve{R}^i_{j'}(\mathrm{w}^{ij})]^{\mathsf{T}}\omega^{ij}\\ &= \frac{1}{2}\begin{bmatrix}1+(\mathrm{w}_1^{ij})^2-(\mathrm{w}_2^{ij})^2 & 2\mathrm{w}_1^{ij}\mathrm{w}_2^{ij} & 2\mathrm{w}_2^{ij}\\ 2\mathrm{w}_1^{ij}\mathrm{w}_2^{ij} & 1-(\mathrm{w}_1^{ij})^2+(\mathrm{w}_2^{ij})^2 & -2\mathrm{w}_1^{ij}\end{bmatrix}\begin{bmatrix}\omega_1^{ij}\\ \omega_2^{ij}\\ \omega_3^{ij}\end{bmatrix},\end{aligned} \tag{20}$$

where $\breve{R}^i_{j'}(\mathrm{w}^{ij})$ is defined as the matrix consisting of the first two columns of the rotation matrix $R^i_{j'}(\mathrm{w}^{ij})$ given in (11).

CHAPTER III

PARTIAL ATTITUDE SYNCHRONIZATION BETWEEN UNDERACTUATED SPACECRAFT TOWARDS A FIXED INERTIAL DIRECTION

3.1 Introduction

The first problem to be addressed is the problem of fixed partial attitude alignment. With each spacecraft having only two of its three principal axes actuated, the orientation of the plane made by these axes, or equivalently, the direction of the third uncontrolled axis, is directly influenced by both control inputs. What is explored in this chapter is therefore the question of aligning the underactuated axis of each spacecraft so that this axis for every spacecraft in the network eventually becomes pointed towards the same direction in inertial space. Specifically, the scenario we consider in this chapter maintains that this final pointing direction is to be fixed in inertial space.

3.2 Problem Definition

Consider the problem of the partial attitude synchronization of N underactuated spacecraft interacting through the communication graph $\mathcal{G}$, which is defined to be a connected and undirected tree. Each spacecraft, denoted by i, belongs to the set $\mathcal{V} = \{1, 2, \ldots, N\}$, and is in communication with (that is, receives state information from) a subset of $\mathcal{V}$ denoted by $\mathcal{N}_i \subset \mathcal{V} \setminus \{i\}$. Since $\mathcal{G}$ is a connected and undirected tree, we have $\mathcal{N}_i \neq \emptyset$ for all $i \in \mathcal{V}$ and that $j \in \mathcal{N}_i$ if and only if $i \in \mathcal{N}_j$.

Recall that the body frame $\hat{\mathbf{b}}^i = (\hat{\mathbf{b}}^i_1, \hat{\mathbf{b}}^i_2, \hat{\mathbf{b}}^i_3)$ is associated with the corresponding spacecraft $i \in \mathcal{V}$. In addition, spacecraft i is assumed to have the principle inertia tensor $I^i = \text{diag}(I^i_1, I^i_2, I^i_3)$, with inertias I^i_1, I^i_2, and I^i_3 along the $\hat{\mathbf{b}}^i_1$, $\hat{\mathbf{b}}^i_2$, and $\hat{\mathbf{b}}^i_3$ axes, respectively. The notation

$$I^i\dot{\omega}^i = S(\omega^i)I^i\omega^i + u^i, \tag{21}$$

refers to the rigid body dynamics specific to spacecraft i, where $u^i = [u_1^i, u_2^i, u_3^i]^\mathsf{T} \in \mathbb{R}^3$ represents the control torque influencing spacecraft i. Accordingly, $\omega^i = [\omega_1^i, \omega_2^i, \omega_3^i]^\mathsf{T} \in \mathbb{R}^3$ represents the inertial angular velocity of spacecraft i expressed in the $\hat{\mathbf{b}}^i$ frame as before, and $S(\cdot)$ represents the skew symmetric matrix representing the cross product between two vectors, i.e., $S(x_1)x_2 = -\overrightarrow{x}_1 \times \overrightarrow{x}_2$.

Each spacecraft $i \in \mathcal{V}$ is underactuated, that is, control torques act only along the $\hat{\mathbf{b}}_1^i$ and $\hat{\mathbf{b}}_2^i$ axes, leaving the $\hat{\mathbf{b}}_3^i$ axis uncontrolled, i.e., $u_3^i \equiv 0$ for all $i \in \mathcal{V}$. The desired objective is to orient the uncontrolled $\hat{\mathbf{b}}_3^i$ axes for each spacecraft so that the final state of $\hat{\mathbf{b}}_3^i$ of each spacecraft is such that they all point along some common, *fixed* inertial direction. This is to be achieved by applying the necessary torques on each spacecraft that depend only on the corresponding *inertial* angular velocities ω^i and the *partial attitude discrepancy* with all communicating spacecraft encoded by w^{ij} for $j \in \mathcal{N}_i$. Henceforth, this objective will be referred to as Problem 1.

3.3 Main Result for Solving Problem 1

In this section, the explicit feedback control law that solves Problem 1 is formulated as a proposition with its analysis given as the proof.

Proposition 1. *Consider a spacecraft network consisting of N spacecraft and assume that the underlying communication graph $\mathcal{G}$ is a tree. The feedback control law*

$$\begin{bmatrix} u_1^i \\ u_2^i \end{bmatrix} = -\sum_{j \in \mathcal{N}_i} k_1^{ij} \mathrm{w}^{ij} - k_2^i \eta^i, \quad i \in \mathcal{V} \tag{22}$$

where $k_1^{ij} = k_1^{ji} > 0$ and $k_2^i > 0$ and where $\eta^i = [\omega_1^i, \omega_2^i]^\mathsf{T} \in \mathbb{R}^2$, ensures that $\lim_{t\to\infty} \mathrm{w}^{ij} = 0$ and $\lim_{t\to\infty} \eta^i = 0$ for all $i \in \mathcal{V}$ and $j \in \mathcal{N}_i$, and thus solves Problem 1.

Proof. From the dynamics (21) and the control law (22), the closed-loop dynamics for each

spacecraft $i \in \mathcal{V}$ is given by

$$\begin{aligned} I_1^i \dot{\omega}_1^i &= (I_2^i - I_3^i)\omega_2^i\omega_3^i - k_2^i\omega_1^i - \sum_{j\in\mathcal{N}_i} k_1^{ij}\mathrm{w}_1^{ij}, \\ I_2^i \dot{\omega}_2^i &= (I_3^i - I_1^i)\omega_1^i\omega_3^i - k_2^i\omega_2^i - \sum_{j\in\mathcal{N}_i} k_1^{ij}\mathrm{w}_2^{ij}, \\ I_3^i \dot{\omega}_3^i &= (I_1^i - I_2^i)\omega_1^i\omega_2^i. \end{aligned} \tag{23}$$

Consider the Lyapunov function candidate

$$V = \sum_{i\in\mathcal{V}}\sum_{j\in\mathcal{N}_i} \frac{1}{2}k_1^{ij}\ln(1+\|\mathrm{w}^{ij}\|^2) + \sum_{i\in\mathcal{V}}\frac{1}{2}(\omega^i)^{\mathsf{T}} I^i \omega^i. \tag{24}$$

Using (18) and (20) along with Lemma 3, the derivative of $\ln(1+\|\mathrm{w}^{ij}\|^2)$ is found as follows.

$$\begin{aligned} \frac{\mathrm{d}}{\mathrm{d}t}\ln(1+\|\mathrm{w}^{ij}\|^2) &= \frac{2}{(1+\|\mathrm{w}^{ij}\|^2)}(\mathrm{w}^{ij})^{\mathsf{T}}\dot{\mathrm{w}}^{ij} \\ &= \frac{2}{(1+\|\mathrm{w}^{ij}\|^2)}\frac{(1+\|\mathrm{w}^{ij}\|^2)}{2}(\mathrm{w}^{ij})^{\mathsf{T}}[\breve{R}^i_{j'}(\mathrm{w}^{ij})]^{\mathsf{T}}\omega^{ij} \\ &= (\tilde{\mathrm{w}}^{ij})^{\mathsf{T}}\omega^{ij} \\ &= (\tilde{\mathrm{w}}^{ij})^{\mathsf{T}}\big(\omega^i - R^i_j\omega^j\big) \\ &= (\tilde{\mathrm{w}}^{ij})^{\mathsf{T}}\omega^i + (\tilde{\mathrm{w}}^{ji})^{\mathsf{T}}\omega^j \\ &= (\mathrm{w}^{ij})^{\mathsf{T}}\eta^i + (\mathrm{w}^{ji})^{\mathsf{T}}\eta^j \end{aligned} \tag{25}$$

Taking now the time derivative of V along the trajectories of (23) yields

$$\begin{aligned} \dot{V} &= \sum_{i\in\mathcal{V}}\sum_{j\in\mathcal{N}_i}\frac{1}{2}k_1^{ij}\frac{2}{(1+\|\mathrm{w}^{ij}\|^2)}(\mathrm{w}^{ij})^{\mathsf{T}}\dot{\mathrm{w}}^{ij} + \sum_{i\in\mathcal{V}}(\omega^i)^{\mathsf{T}}I^i\dot{\omega}^i \\ &= \sum_{i\in\mathcal{V}}\sum_{j\in\mathcal{N}_i}\frac{1}{2}k_1^{ij}\Big((\mathrm{w}^{ij})^{\mathsf{T}}\eta^i + (\mathrm{w}^{ji})^{\mathsf{T}}\eta^j\Big) - \sum_{i\in\mathcal{V}}\sum_{j\in\mathcal{N}_i}k_1^{ij}(\eta^i)^{\mathsf{T}}\mathrm{w}^{ij} - \sum_{i\in\mathcal{V}}k_2^i(\eta^i)^{\mathsf{T}}\eta^i \\ &= \sum_{i\in\mathcal{V}}\sum_{j\in\mathcal{N}_i}\frac{1}{2}k_1^{ij}2(\mathrm{w}^{ij})^{\mathsf{T}}\eta^i - \sum_{i\in\mathcal{V}}\sum_{j\in\mathcal{N}_i}k_1^{ij}(\eta^i)^{\mathsf{T}}\mathrm{w}^{ij} - \sum_{i\in\mathcal{V}}k_2^i(\eta^i)^{\mathsf{T}}\eta^i \\ &= \sum_{i\in\mathcal{V}}\sum_{j\in\mathcal{N}_i}k_1^{ij}\Big((\mathrm{w}^{ij})^{\mathsf{T}}\eta^i - (\eta^i)^{\mathsf{T}}\mathrm{w}^{ij}\Big) - \sum_{i\in\mathcal{V}}k_2^i(\eta^i)^{\mathsf{T}}\eta^i \\ &= -\sum_{i\in\mathcal{V}}k_2^i(\eta^i)^{\mathsf{T}}\eta^i \;\leq\; 0. \end{aligned} \tag{26}$$

It follows that the system is Lyapunov stable and hence w^{ij} and ω^i for all $i \in \mathcal{V}$, $j \in \mathcal{N}_i$, are bounded. From (23), it follows that $\mathcal{M} \triangleq \{(\mathrm{w}^{ij}, \eta^i) : \dot{V} \equiv 0\} = \{(\mathrm{w}^{ij}, 0) : \sum_{j\in\mathcal{N}_i} k_1^{ij}\mathrm{w}^{ij} = 0,\ \forall i \in \mathcal{V}\}$.

Since an undirected tree with N vertices and $M = N - 1$ edges has an incidence matrix $\mathcal{D}(\mathcal{G}) \in \mathbb{R}^{N \times M}$ that is full column rank [16], the agreement subspace $\lim_{t\to\infty} \sum_{j\in\mathcal{N}_i} k_1^{ij} \mathrm{w}^{ij} = 0$ for all $i \in \mathcal{V}$ can be described as

$$\begin{bmatrix} \sum_{j\in\mathcal{N}_1} k_1^{1j} \mathrm{w}^{1j} \\ \vdots \\ \sum_{j\in\mathcal{N}_N} k_1^{Nj} \mathrm{w}^{Nj} \end{bmatrix} = \mathbf{0} = \tilde{\mathcal{D}}(\mathcal{G}) W, \tag{27}$$

where the edges $\varepsilon_e \in \mathcal{E}$, $e = 1, \cdots, M$, have been directed such that the resulting graph forms an arborescence, $\tilde{\mathcal{D}}(\mathcal{G}) \in \mathbb{R}^{2N \times 2M}$ is a block matrix with the same form as $\mathcal{D}(\mathcal{G}) \otimes A$, where $A \in \mathbb{R}^{2\times 2}$, and $W \in \mathbb{R}^{2M}$ is a vector containing the w parameters. Accordingly, $\tilde{\mathcal{D}}(\mathcal{G})$ is constructed as

$$[\tilde{\mathcal{D}}(\mathcal{G})]_{\alpha,\beta} = \begin{cases} \mathrm{I}_{2\times 2} & \text{if } (j,i) = \varepsilon_e \in \mathcal{E}, \\ -\tilde{R}_j^i & \text{if } (i,j) = \varepsilon_e \in \mathcal{E}, \\ 0 & \text{otherwise,} \end{cases} \tag{28}$$

and W is constructed as

$$[W]_\beta = k_1^{ij} \mathrm{w}^{ij}, \quad \text{if } (j,i) = \varepsilon_e \in \mathcal{E}, \tag{29}$$

where α and β indicate a range of indices for the submatrix $[\tilde{\mathcal{D}}(\mathcal{G})]_{\alpha,\beta}$ and the subvector $[W]_\beta$ where $2i - 1 \leq \alpha \leq 2i$ and $2e - 1 \leq \beta \leq 2e$.

It follows from Lemma 2 and Lemma 3 that $\tilde{\mathcal{D}}(\mathcal{G})$ is full column rank, $W = 0$, and $\mathrm{w}^{ij} = 0$ for all $i \in \mathcal{V}, j \in \mathcal{N}_i$. Thus, the agreement subspace $\mathcal{M}$ consists only of the point $\mathrm{w}^{ij} = 0$ and $\eta^i = 0$ for all $i \in \mathcal{V}, j \in \mathcal{N}_i$. By LaSalle's invariance principle, the proof is complete. □

The solution given here to solve Problem 1 takes the form of a linear controller and is capable of achieving almost global asymptotic stability with respect to the partial consensus state. The locations in $SO(3)$ for which the solution breaks down is only a single point where the w parameters reach infinity. This arises when the underactuated axes of two spacecraft who are neighbors of each other point in the exact opposite direction in the inertial space, and is a consequence of the stereographic projection of each of these axes in the others' frame

of reference which the formulation of the w parameters are based upon. Since the proof of Proposition 1 includes boundedness of the state, then all that is necessary in avoiding the breakdown of the solution is ensuring the system does have as initial conditions two neighboring spacecraft pointing their uncontrolled axes opposite to each other.

The conclusion that the solution provides almost global asymptotic stability hinges upon the LaSalle argument stemming from the analysis of (27). To exemplify the use of Lemma 2 in the proof, consider a network of four spacecraft so that $\mathcal{V} = \{1, 2, 3, 4\}$ and its communication topology is encoded in the sets $\mathcal{N}_i$, for $i \in \mathcal{V}$, where $\mathcal{N}_1 \triangleq \{3\}$, $\mathcal{N}_2 \triangleq \{3\}$, $\mathcal{N}_3 \triangleq \{1, 2, 4\}$, $\mathcal{N}_4 \triangleq \{3\}$ as shown in Fig. 4.

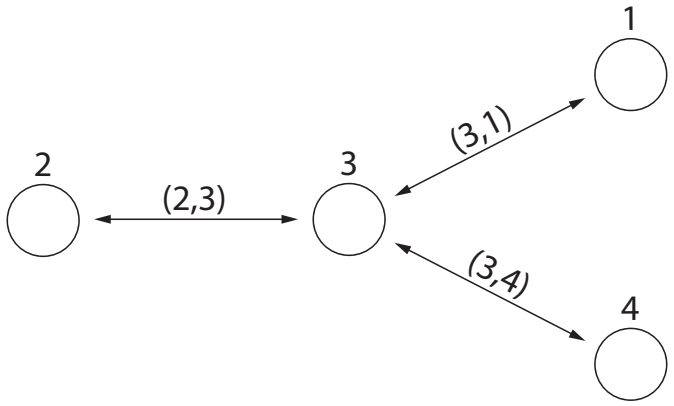

Figure 4: Example communication graph with undirected edges.

If the nodes are relabeled and edges directed as perscribed in Lemma 1, one possibility for the resulting graph may be what is shown in Fig. 5.

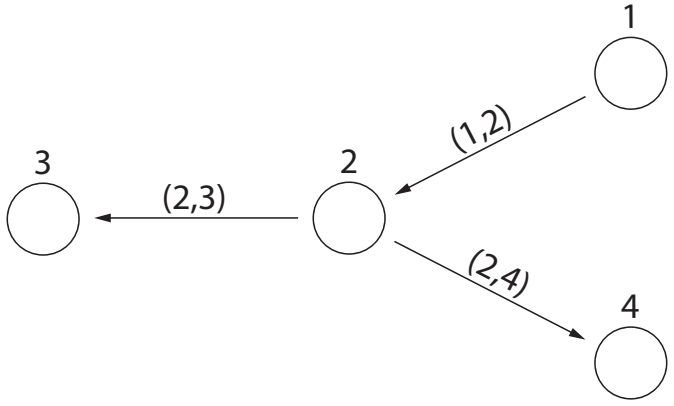

Figure 5: Example communication graph with relabeled nodes and directed edges.

The application of Lemma 2 then can be used to transform the rearranged graph's corresponding incidence matrix $\mathcal{D}(\mathcal{G})$ to the incidence-like matrix $\tilde{\mathcal{D}}(\mathcal{G})$, which is constructed similarly to what is specified in the proof and is given below

$$\mathcal{D}(\mathcal{G}) = \begin{bmatrix} -1 & 0 & 0 \\ 1 & -1 & -1 \\ 0 & 1 & 0 \\ 0 & 0 & 1 \end{bmatrix} \quad \Rightarrow \quad \tilde{\mathcal{D}}(\mathcal{G}) = \begin{bmatrix} -\tilde{R}_2^1 & 0 & 0 \\ \mathrm{I}_{2\times 2} & -\tilde{R}_3^2 & -\tilde{R}_4^2 \\ 0 & \mathrm{I}_{2\times 2} & 0 \\ 0 & 0 & \mathrm{I}_{2\times 2} \end{bmatrix}, \tag{30}$$

with the vector containing the w parameters being $W = [k_1^{21}\mathrm{w}^{21}, k_1^{32}\mathrm{w}^{32}, k_1^{42}\mathrm{w}^{42}]^\mathsf{T}$ for this example. It is easy to see that, after applying Lemma 3, this is precisely what would be provided by (27). The fact that the matrix $\tilde{\mathcal{D}}(\mathcal{G})$ is full column rank follows immediately.

3.4 Simulation 1: 4-Spacecraft Network With Inertial Velocity Feedback

As a demonstration of the effectiveness of the proposed control law, consider again the system with four spacecraft mentioned earlier. It is assumed that the spacecraft communication topology is encoded in the sets $\mathcal{N}_i$, for $i \in \mathcal{V} = \{1, 2, 3, 4\}$, where $\mathcal{N}_1 \triangleq \{3\}$, $\mathcal{N}_2 \triangleq \{3\}$, $\mathcal{N}_3 \triangleq \{1, 2, 4\}$, $\mathcal{N}_4 \triangleq \{3\}$, the same topology depicted in Fig. 4. The spacecraft are all underactuated so that the $\hat{\mathbf{b}}_3^i$ principal axis of each spacecraft $i \in \mathcal{V}$ is uncontrolled, and they possess moments of inertia $I^1 = \mathrm{diag}(45, 25, 15)$ kg $\cdot$ m^2, $I^2 = \mathrm{diag}(15, 35, 45)$ kg $\cdot$ m^2, $I^3 = \mathrm{diag}(84, 24, 15)$ kg $\cdot$ m^2, and $I^4 = \mathrm{diag}(60, 40, 15)$ kg $\cdot$ m^2 for Spacecraft 1, 2, 3, and 4, respectively. The initial orientations given in unit quaternions and the initial angular velocities for Spacecraft 1, 2, 3, and 4 were chosen as

$$q_1 = \begin{bmatrix} 0.9397 \\ 0 \\ 0.3420 \\ 0 \end{bmatrix}, \quad q_2 = \begin{bmatrix} 0.6161 \\ 0.3315 \\ -0.0709 \\ 0.7110 \end{bmatrix}, \quad q_3 = \begin{bmatrix} 0 \\ -0.6216 \\ 0 \\ 0.7833 \end{bmatrix}, \quad q_4 = \begin{bmatrix} 0 \\ 0.7262 \\ 0 \\ -0.6875 \end{bmatrix}, \tag{31}$$

and

$$\omega^1(0) = \begin{bmatrix} 0.2 \\ -0.1 \\ 0.1 \end{bmatrix} \frac{\text{rad}}{\text{s}}, \quad \omega^2(0) = \begin{bmatrix} -0.1 \\ -0.1 \\ -0.2 \end{bmatrix} \frac{\text{rad}}{\text{s}}, \quad \omega^3(0) = \begin{bmatrix} 0.1 \\ 0.1 \\ 0.1 \end{bmatrix} \frac{\text{rad}}{\text{s}}, \quad \omega^4(0) = \begin{bmatrix} 0.1 \\ 0.3 \\ 0.1 \end{bmatrix} \frac{\text{rad}}{\text{s}}, \tag{32}$$

respectively, with the control gains set to $k_1 = 0.2$ and $k_2^i = 1$ for $i = 1, 2, 3, 4$.

The w parameters describing the $\hat{\mathbf{b}}_3$ axis of Spacecraft 2 in the frame of Spacecraft 1 and Spacecraft 1, 2, and 4 in the frame of Spacecraft 3, and so describe some "distance" from consensus, are plotted in Fig. 6. Similar behavior exists from the results for the other partial attitude parameters as well. In order to visually confirm the outcome of applying the control law to solve Problem 1, an animation from the simulation was created depicting the spacecraft as they rotate in inertial space, and several snapshots of various phases of the simulation are shown in Fig. 7.

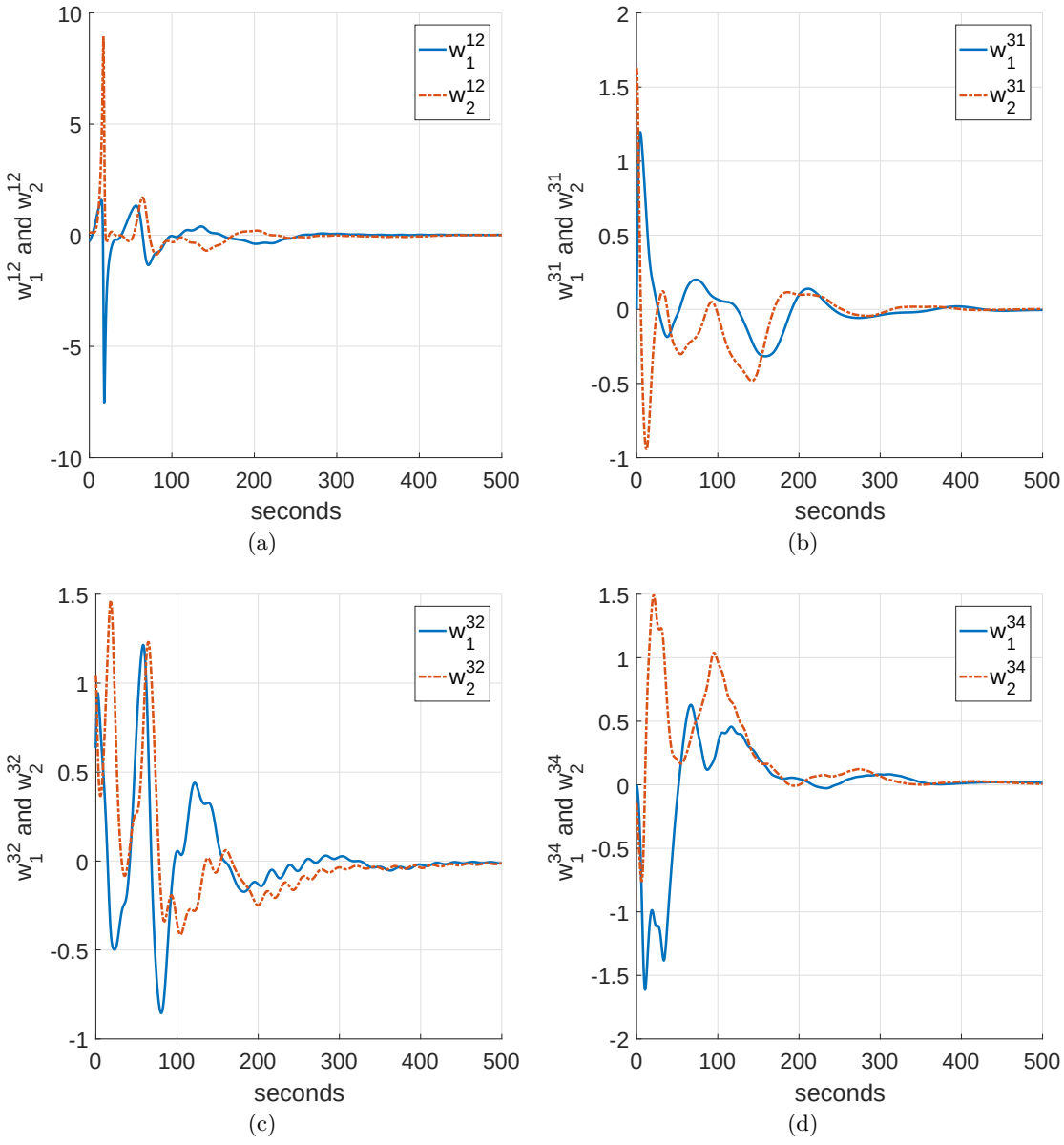

Figure 6: The w parameter state histories for Problem 1: (a) w parameters of Spacecraft 2 in the frame of Spacecraft 1; (b) w parameters of Spacecraft 1 in the frame of Spacecraft 3; (c) w parameters of Spacecraft 2 in the frame of Spacecraft 3; (d) w parameters of Spacecraft 4 in the frame of Spacecraft 3.

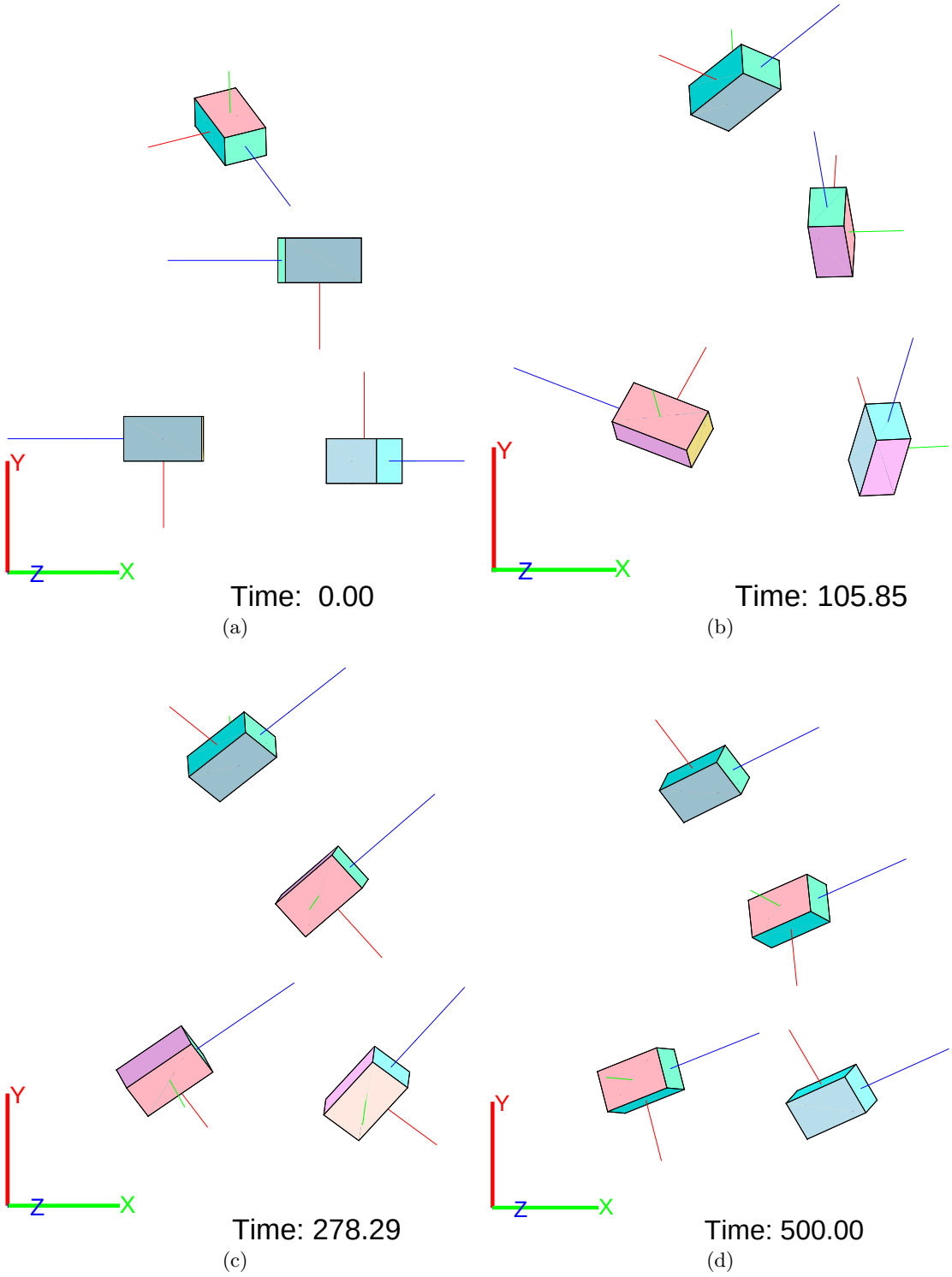

Figure 7: Snapshots at different phases of the simulation for Problem 1.

CHAPTER IV

PARTIAL ATTITUDE SYNCHRONIZATION BETWEEN UNDERACTUATED SPACECRAFT USING RELATIVE VELOCITY FEEDBACK

4.1 Introduction

Similar to the previous chapter, the objective here is to align the uncontrolled $\hat{\mathbf{b}}_3^i$ axes of all spacecraft so that they are aligned and point in the same direction in inertial space. The difference between what is explored in this chapter compared to Chapter 3 consists of two ideas. One being that the final pointing direction of the uncontrolled axes arriving to a fixed state in inertial space is not directly enforced. Instead, this direction is intended to be left free so that it may be allowed to rotate in the inertial frame. The other is to remove the control law's reliance upon inertial information about neighboring spacecraft, and instead, utilize only relative state information as measured in the frame of the acting control. Using relative state information in the control law removes the need for explicit knowledge of both the inertial orientation of the spacecraft it is influencing and the inertial orientation and inertial velocities of the neighboring spacecraft. This implies that a communication link between the spacecraft is not entierly necessary, and as an alternative, this relative information may be gathered via on-board cameras, for example.

4.2 Problem Definition

This chapter involves the partial synchronization of an N-spacecraft cluster, where the final pointing direction of the uncontrolled axes is the same for all spacecraft, but may not be fixed in inertial space. Following suit with the naming in the previous chapter, the problem considered here shall henceforth be referred to as Problem 2. We assume that the communication graph $\mathcal{G}$ has the same properties as given for Problem 1, that is, the graph $\mathcal{G}$ is a connected and undirected tree.

The desired objective of Problem 2 is to find a distributed control law which will synchronize the uncontrolled $\hat{\mathbf{b}}_3^i$ axes for all spacecraft so that the final orientation of $\hat{\mathbf{b}}_3^i$ for each spacecraft $i \in \mathcal{V}$ is along some common inertial direction. This can be achieved by applying the necessary torques to each spacecraft $i \in \mathcal{V}$ that depend upon the *partial relative angular velocities* defined as

$$\eta^{ij} = \eta^i - \tilde{R}_j^i \eta^j, \quad j \in \mathcal{N}_i, \tag{33}$$

where $\tilde{R}_j^i \in \mathbb{R}^{2\times 2}$ represents the upper left 2×2 submatrix of R_j^i, and the *partial attitude discrepancy* between described by w^{ij} for $j \in \mathcal{N}_i$, and the inertia tensor I^i.

Next, we present a lemma that will help us solve Problem 2.

Lemma 4. *Let Q_i represent the rotation matrix that transforms elements from the body frame $\hat{\mathbf{b}}^i$ to the inertial frame, let $\breve{Q}_i \in \mathbb{R}^{3\times 2}$ be the matrix consisting of the first two columns of Q_i, and let Q_j and $\breve{Q}_j$ be defined similarly for the body frame $\hat{\mathbf{b}}^j$. Then, $\breve{Q}_i^{\mathsf{T}} \breve{Q}_i = \mathrm{I}_2$ and $\breve{Q}_i^{\mathsf{T}} \breve{Q}_j = \tilde{R}_j^i$.*

Proof. The proof follows immediately by performing the corresponding matrix multiplications, and thus it is omitted. □

4.3 Main Result for Solving Problem 2

In this section, the explicit feedback control law that solves Problem 2 is formulated as a proposition with its analysis given as the proof.

Proposition 2. *Consider a network consisting of N spacecraft, and assume that the corresponding communication graph $\mathcal{G}$ is a tree. Let the feedback control law for each spacecraft $i \in \mathcal{V}$ be given by*

$$\begin{bmatrix} u_1^i \\ u_2^i \end{bmatrix} = -k_3^i \begin{bmatrix} (I_2^i - I_3^i)\omega_2^i \omega_3^i \\ (I_3^i - I_1^i)\omega_1^i \omega_3^i \end{bmatrix} - \sum_{j\in\mathcal{N}_i} k_1 \mathrm{w}^{ij} - \sum_{j\in\mathcal{N}_i} k_2 \eta^{ij}, \tag{34}$$

where $k_1 > 0$, $k_2 > 0$, and

$$k_3^i = \begin{cases} 1 & \text{for } I_1^i \neq I_2^i, \\ \mu_i & \text{for } I_1^i = I_2^i, \end{cases} \tag{35}$$

where $\mu_i \in \mathbb{R}$. *The previous control ensures that* $\lim_{t\to\infty} \mathrm{w}^{ij} = 0$ *and* $\lim_{t\to\infty} \eta^{ij} = 0$, *and thus solves Problem 2.*

Proof. From the dynamics (21) and the control law (34), the closed-loop dynamics of each spacecraft $i \in \mathcal{V}$ is given by

$$\begin{aligned} I_1^i\dot{\omega}_1^i &= (1-k_3^i)(I_2^i - I_3^i)\omega_2^i\omega_3^i - \sum_{j\in\mathcal{N}_i} k_1 \mathrm{w}_1^{ij} - \sum_{j\in\mathcal{N}_i} k_2\eta_1^{ij}, \\ I_2^i\dot{\omega}_2^i &= (1-k_3^i)(I_3^i - I_1^i)\omega_1^i\omega_3^i - \sum_{j\in\mathcal{N}_i} k_1 \mathrm{w}_2^{ij} - \sum_{j\in\mathcal{N}_i} k_2\eta_2^{ij}, \\ I_3^i\dot{\omega}_3^i &= (I_1^i - I_2^i)\omega_1^i\omega_2^i. \end{aligned} \tag{36}$$

Consider the Lyapunov function candidate

$$V = \sum_{i\in\mathcal{V}}\sum_{j\in\mathcal{N}_i} \frac{1}{2} k_1 \ln(1 + \|\mathrm{w}^{ij}\|^2) + \sum_{i\in\mathcal{V}} \frac{1}{2}(\eta^i)^{\mathsf{T}} J^i \eta^i, \tag{37}$$

where $J^i = \mathrm{diag}(I_1^i, I_2^i)$. Taking the derivative of V along the trajectories of (36) and using (25), (33), and Lemma 4 yields

$$\begin{aligned} \dot{V} &= \sum_{i\in\mathcal{V}}\sum_{j\in\mathcal{N}_i} \frac{1}{2} k_1 \frac{2}{1+\|\mathrm{w}^{ij}\|^2} (\mathrm{w}^{ij})^{\mathsf{T}} \dot{\mathrm{w}}^{ij} + \sum_{i\in\mathcal{V}} (\eta^i)^{\mathsf{T}} J^i \dot{\eta}^i \\ &= \sum_{i\in\mathcal{V}}\sum_{j\in\mathcal{N}_i} \frac{1}{2} k_1 \left((\mathrm{w}^{ij})^{\mathsf{T}}\eta^i + (\mathrm{w}^{ji})^{\mathsf{T}}\eta^j \right) - \sum_{i\in\mathcal{V}}\sum_{j\in\mathcal{N}_i} k_1 (\eta^i)^{\mathsf{T}} \mathrm{w}^{ij} - \sum_{i\in\mathcal{V}}\sum_{j\in\mathcal{N}_i} k_2 (\eta^i)^{\mathsf{T}}\eta^{ij} \\ &= \sum_{i\in\mathcal{V}}\sum_{j\in\mathcal{N}_i} \frac{1}{2} k_1 2 (\mathrm{w}^{ij})^{\mathsf{T}}\eta^i - \sum_{i\in\mathcal{V}}\sum_{j\in\mathcal{N}_i} k_1 (\eta^i)^{\mathsf{T}} \mathrm{w}^{ij} - \sum_{i\in\mathcal{V}}\sum_{j\in\mathcal{N}_i} k_2 (\eta^i)^{\mathsf{T}}\eta^{ij} \\ &= \sum_{i\in\mathcal{V}}\sum_{j\in\mathcal{N}_i} k_1 \left((\mathrm{w}^{ij})^{\mathsf{T}}\eta^i - (\eta^i)^{\mathsf{T}} \mathrm{w}^{ij} \right) - \sum_{i\in\mathcal{V}}\sum_{j\in\mathcal{N}_i} k_2 (\eta^i)^{\mathsf{T}}\eta^{ij} \\ &= -\sum_{i\in\mathcal{V}}\sum_{j\in\mathcal{N}_i} k_2 (\eta^i)^{\mathsf{T}}\eta^{ij} \\ &= -k_2 \sum_{i\in\mathcal{V}}\sum_{j\in\mathcal{N}_i} (\eta^i)^{\mathsf{T}} \left(\eta^i - \tilde{R}_j^i \eta^j \right) \\ &= -k_2 \sum_{i\in\mathcal{V}}\sum_{j\in\mathcal{N}_i} (\eta^i)^{\mathsf{T}} \left(\breve{Q}_i^{\mathsf{T}} \breve{Q}_i \eta^i - \breve{Q}_i^{\mathsf{T}} \breve{Q}_j \eta^j \right) \\ &= -k_2 \sum_{i\in\mathcal{V}}\sum_{j\in\mathcal{N}_i} (\breve{Q}_i\eta^i)^{\mathsf{T}} \left(\breve{Q}_i \eta^i - \breve{Q}_j \eta^j \right) \\ &= -k_2 \mathcal{H}^{\mathsf{T}} \tilde{\mathcal{L}}(\mathcal{G}) \mathcal{H} \leq 0 \end{aligned} \tag{38}$$

where $\mathcal{H} = [(\breve{Q}_1\eta^1)^{\mathsf{T}}, \cdots, (\breve{Q}_N\eta^N)^{\mathsf{T}}]^{\mathsf{T}} \in \mathbb{R}^{3N}$, $\tilde{\mathcal{L}}(\mathcal{G}) = \mathcal{L}(\mathcal{G}) \otimes \mathrm{I}_{3\times 3}$, and $\mathcal{L}(\mathcal{G})$ is the graph Laplacian. Since $\dot{V} \leq 0$, it follows that the signals w^{ij} and η^i for all $i \in \mathcal{V}$, $j \in \mathcal{N}_i$, are

bounded. Letting $\dot{V} \equiv 0$, from the properties of $\mathcal{L}(\mathcal{G})$, it follows that the null space of $\tilde{\mathcal{L}}(\mathcal{G})$ is $\mathbf{1}_N \otimes y$ where $y \in \mathbb{R}^3$, and thus $\breve{Q}_i \eta^i = y$ for all $i \in \mathcal{V}$. This implies that $\dot{V} = 0$ if and only if

$$\breve{Q}_i \eta^i = \breve{Q}_j \eta^j, \quad \forall i, j \in \mathcal{V} \tag{39}$$

which after a left multiplication by $\breve{Q}_i^{\mathsf{T}}$, and using again Lemma 4, yields that $\eta^i = \tilde{R}_j^i \eta^j$ for all $i, j \in \mathcal{V}$. Along with (39), this leads to

$$\eta^{ij} = \eta^i - \tilde{R}_j^i \eta^j = 0, \quad \forall i, j \in \mathcal{V} \tag{40}$$

indicating that $\mathcal{M} \triangleq \{(\mathrm{w}^{ij}, \eta^{ij}) : \dot{V} \equiv 0\} = \{(\mathrm{w}^{ij}, 0),\ \forall i \in \mathcal{V},\ j \in \mathcal{N}_i\}$. Furthermore, note that (40) implies that

$$(\eta^i)^{\mathsf{T}} \eta^i = (\eta^j)^{\mathsf{T}} \eta^j, \quad \forall i, j \in \mathcal{V} \tag{41}$$

and thus the following series of equations hold:

$$\begin{aligned}
0 &= (\eta^j)^{\mathsf{T}} \eta^j - (\eta^j)^{\mathsf{T}} \eta^j \\
&= (\eta^j)^{\mathsf{T}} \eta^j - (\eta^i)^{\mathsf{T}} (\tilde{R}_i^j)^{\mathsf{T}} \tilde{R}_i^j \eta^i \\
&= (\eta^j)^{\mathsf{T}} \eta^j - (\eta^i)^{\mathsf{T}} \tilde{R}_j^i (\tilde{R}_j^i)^{\mathsf{T}} \eta^i \\
&= (\eta^j)^{\mathsf{T}} \eta^j - (\eta^i)^{\mathsf{T}} \eta^i + \frac{4}{(1 + \|\mathrm{w}^{ij}\|^2)^2} (\omega_1^i \mathrm{w}_2^{ij} - \omega_2^i \mathrm{w}_1^{ij}) \\
&= \omega_1^i \mathrm{w}_2^{ij} - \omega_2^i \mathrm{w}_1^{ij}, \quad \forall i, j \in \mathcal{V}.
\end{aligned} \tag{42}$$

Assume now that $\mathrm{w}^{ij} \neq 0$ for some $i \in \mathcal{V}$, $j \in \mathcal{N}_i$, otherwise there is nothing to prove (this comes from the fact that at this point in the proof, $\eta^{ij} = 0$ for all $i \in \mathcal{V}$, $j \in \mathcal{N}_i$, and so if in addition $\mathrm{w}^{ij} = 0$ for every $i \in \mathcal{V}$, $j \in \mathcal{N}_i$, then the successful partial synchronization of the spacecraft network is achieved). Also assume that $\eta^i \neq 0$ for all $i \in \mathcal{V}$ (since if $\eta^i \neq 0$ for some $i \in \mathcal{V}$, then since $\breve{Q}_i$ is full column rank, it follows from (39) that $\eta^i \neq 0$ for all $i \in \mathcal{V}$), otherwise, $\eta^i = 0$ for all $i \in \mathcal{V}$, and (36) indicates $\sum_{j \in \mathcal{N}_i} \mathrm{w}^{ij} = 0$ for all $i \in \mathcal{V}$, in which case the proof is completed using an argument similar to what is given in the proof of Problem 1. From (42), it then follows that

$$\mathrm{w}^{ij} = \lambda_{ij} \eta^i, \quad \forall i, j \in \mathcal{V} \tag{43}$$

where $\lambda_{ij} \neq 0$ for some $i \in \mathcal{V}$, $j \in \mathcal{N}_i$. Next, let $\mathrm{w}^{ji} = \lambda_{ji}\eta^j$ and notice that left multiplying (43) with $\tilde{R}_i^j$ leads to $-\mathrm{w}^{ji} = \lambda_{ij}\eta^j$, where Lemma 3 and (40) were used. This implies that for each communication path between i and j, $i \in \mathcal{V}$, $j \in \mathcal{N}_i$, the proportionality constant in $\mathrm{w}^{ij} = \lambda_{ij}\eta^i$ and $\mathrm{w}^{ji} = \lambda_{ji}\eta^j$ are equal and opposite ($\lambda_{ij} = -\lambda_{ji}$) and thus a single constant $\lambda_{ij} = -\lambda_{ji} = \lambda_e$ may be associated with each undirected edge $(i,j) = \varepsilon_e \in \mathcal{E}$.

Letting $\sum_{j\in\mathcal{N}_i} \lambda_{ij} = \Lambda_i$, it follows that $\sum_{j\in\mathcal{N}_i} \mathrm{w}^{ij} = \sum_{j\in\mathcal{N}_i} \lambda_{ij}\eta^i = \Lambda_i\eta^i$. The relationship between the vectors constructed by $\Gamma = [\Lambda_1, \cdots, \Lambda_N]^\mathsf{T} \in \mathbb{R}^N$ and $\gamma = [\lambda_1, \cdots, \lambda_M]^\mathsf{T} \in \mathbb{R}^M$, with M being the number of edges in the graph $\mathcal{G}$, can then be expressed as

$$\Gamma = \mathcal{D}(\mathcal{G})\gamma \tag{44}$$

where $\mathcal{D}(\mathcal{G})$ is the incidence matrix for the communication graph $\mathcal{G}$. Since $\mathcal{G}$ is a tree (i.e. $\mathcal{D}(\mathcal{G})$ is full column rank) and at least one $\lambda_e \neq 0$, $\varepsilon_e \in \mathcal{E}$, there are at least two $\Lambda_i \neq 0$, $i \in \mathcal{V}$. By taking the derivative of (41) and using (40) and (43), one obtains

$$\begin{aligned}
(\eta^i)^\mathsf{T}\dot{\eta}^i &= (\eta^p)^\mathsf{T}\dot{\eta}^p, \\
(\eta^i)^\mathsf{T}\left((1-k_3^i)\tilde{S}^i\omega_3^i - \sum_{j\in\mathcal{N}_i} k_1\mathrm{w}^{ij}\right) &= (\eta^p)^\mathsf{T}\left((1-k_3^p)\tilde{S}^p\omega_3^p - \sum_{q\in\mathcal{N}_p} k_1\mathrm{w}^{pq}\right) \\
-(\eta^i)^\mathsf{T}(J^i)^{-1}k_1\sum_{j\in\mathcal{N}_i}\mathrm{w}^{ij} &= -(\eta^p)^\mathsf{T}(J^p)^{-1}k_1\sum_{q\in\mathcal{N}_p}\mathrm{w}^{pq}, \\
-\Lambda_i k_1(\eta^i)^\mathsf{T}(J^i)^{-1}\eta^i &= -\Lambda_p k_1(\eta^p)^\mathsf{T}(J^p)^{-1}\eta^p,
\end{aligned} \tag{45}$$

where

$$\tilde{S}^i = \begin{bmatrix} (I_2^i - I_3^i)\omega_2^i/I_1^i \\ (I_3^i - I_1^i)\omega_1^i/I_2^i \end{bmatrix}, \quad \tilde{S}^p = \begin{bmatrix} (I_2^p - I_3^p)\omega_2^p/I_1^p \\ (I_3^p - I_1^p)\omega_1^p/I_2^p \end{bmatrix}, \tag{46}$$

and $i, p \in \mathcal{V}$. Since $-k_1(\eta^i)^\mathsf{T}(J^i)^{-1}\eta^i < 0$ for all $i \in \mathcal{V}$ and since at least one $\Lambda_i \neq 0$, $i \in \mathcal{V}$, then it follows necessarily that

$$\Lambda_i \neq 0, \ \ \forall i \in \mathcal{V}, \tag{47a}$$

$$\mathrm{sign}(\Lambda_i) = \mathrm{sign}(\Lambda_p), \ \ \forall i, p \in \mathcal{V}, \tag{47b}$$

Using property (4), the following can be easily shown.

$$\begin{aligned}
\left(\mathrm{I}_N - \mathcal{D}(\mathcal{G})\mathcal{D}^+(\mathcal{G})\right)\Gamma &= \frac{1}{N}\mathbf{1}_{N\times N}\Gamma \\
\mathrm{I}_N\Gamma - \mathcal{D}(\mathcal{G})\mathcal{D}^+(\mathcal{G})\Gamma &= \frac{1}{N}\mathbf{1}_{N\times N}\Gamma \\
\Gamma - \mathcal{D}(\mathcal{G})\gamma &= \frac{1}{N}\mathbf{1}_{N\times N}\Gamma \\
\Gamma - \Gamma &= \frac{1}{N}\mathbf{1}_{N\times N}\Gamma \\
\mathbf{0} &= \frac{1}{N}\mathbf{1}_{N\times N}\Gamma
\end{aligned} \tag{48}$$

However, due to (47a) and (47b), it follows that $\frac{1}{N}\mathbf{1}_{N\times N}\Gamma \neq 0$, leading to a contradiction. Thus, necessarily $\Lambda_i = 0$ for all $i \in \mathcal{V}$.

Since $\mathcal{D}(\mathcal{G})$ is full column rank and $\Gamma = \mathbf{0}$, it follows from (44) that $\lambda_e = 0$ for all $(i,j) = \varepsilon_e \in \mathcal{E}$ which violates our assumption in (43). Since $\lambda_e = 0$ for all $(i,j) = \varepsilon_e \in \mathcal{E}$, it follows that $\mathrm{w}^{ij} = 0$ for all $i \in \mathcal{V}$, $j \in \mathcal{N}_i$. Thus, the agreement subspace $\mathcal{M}$ consists only of the point where $\mathrm{w}^{ij} = 0$ and $\eta^{ij} = 0$ for all $i \in \mathcal{V}, j \in \mathcal{N}_i$. By LaSalle's invariance principle, the proof is complete. □

4.3.1 Simulation 2: 4-Spacecraft Network With Relative Velocity Feedback

To demonstrate the effectiveness of the control law which solves Problem 2, consider once again the system with four spacecraft mentioned earlier. It is assumed that the spacecraft communication topology is encoded in the sets $\mathcal{N}_i$, for $i \in \mathcal{V} = \{1,2,3,4\}$, where $\mathcal{N}_1 \triangleq \{3\}$, $\mathcal{N}_2 \triangleq \{3\}$, $\mathcal{N}_3 \triangleq \{1,2,4\}$, $\mathcal{N}_4 \triangleq \{3\}$, the same topology used in the simulation for Problem 1 and depicted in Fig. 4. The spacecraft are all underactuated so that the $\hat{\mathbf{b}}_3^i$ principal axis of each spacecraft $i \in \mathcal{V}$ is uncontrolled, and they possess moments of inertia $I^1 = \mathrm{diag}(25,25,15)\ \mathrm{kg}\cdot\mathrm{m}^2$, $I^2 = \mathrm{diag}(15,35,45)\ \mathrm{kg}\cdot\mathrm{m}^2$, $I^3 = \mathrm{diag}(34,24,15)\ \mathrm{kg}\cdot\mathrm{m}^2$, and $I^4 = \mathrm{diag}(30,40,15)\ \mathrm{kg}\cdot\mathrm{m}^2$ for Spacecraft 1, 2, 3, and 4, respectively. The initial orientations given in unit quaternions and the initial angular velocities for Spacecraft 1, 2,

3, and 4 were chosen as

$$q_1 = \begin{bmatrix} 1 \\ 0 \\ 0 \\ 0 \end{bmatrix}, \quad q_2 = \begin{bmatrix} 0.5547 \\ 0.5547 \\ -0.2774 \\ 0.5547 \end{bmatrix}, \quad q_3 = \begin{bmatrix} 0 \\ -0.3162 \\ 0 \\ 0.9487 \end{bmatrix}, \quad q_4 = \begin{bmatrix} 0 \\ -0.4472 \\ 0 \\ 0.8944 \end{bmatrix}, \tag{49}$$

and

$$\omega^1(0) = \begin{bmatrix} 0.2 \\ -0.1 \\ 0.1 \end{bmatrix} \frac{\text{rad}}{\text{s}}, \quad \omega^2(0) = \begin{bmatrix} -0.1 \\ -0.1 \\ -0.2 \end{bmatrix} \frac{\text{rad}}{\text{s}}, \quad \omega^3(0) = \begin{bmatrix} 0.1 \\ 0.1 \\ 0.3 \end{bmatrix} \frac{\text{rad}}{\text{s}}, \quad \omega^4(0) = \begin{bmatrix} 0.1 \\ 0.3 \\ 0.1 \end{bmatrix} \frac{\text{rad}}{\text{s}}, \tag{50}$$

respectively, with the control gains set to $k_1 = 1.5$, $k_2 = 2$, $k_3^1 = 0$, and $k_3^i = 1$ for $i = 2, 3, 4$.

The w parameters describing the $\hat{\mathbf{b}}_3$ axis of Spacecraft 2 in the frame of Spacecraft 1 and Spacecraft 1, 2, and 4 in the frame of Spacecraft 3 are plotted in Fig. 8. Similar behavior was observed for the other partial attitude parameters as well. To aid in visually confirming the outcome of applying the control law to solve Problem 2, an animation from the simulation was created depicting the spacecraft as they rotate in inertial space, and several snapshots of various phases of the simulation are shown in Fig. 9.

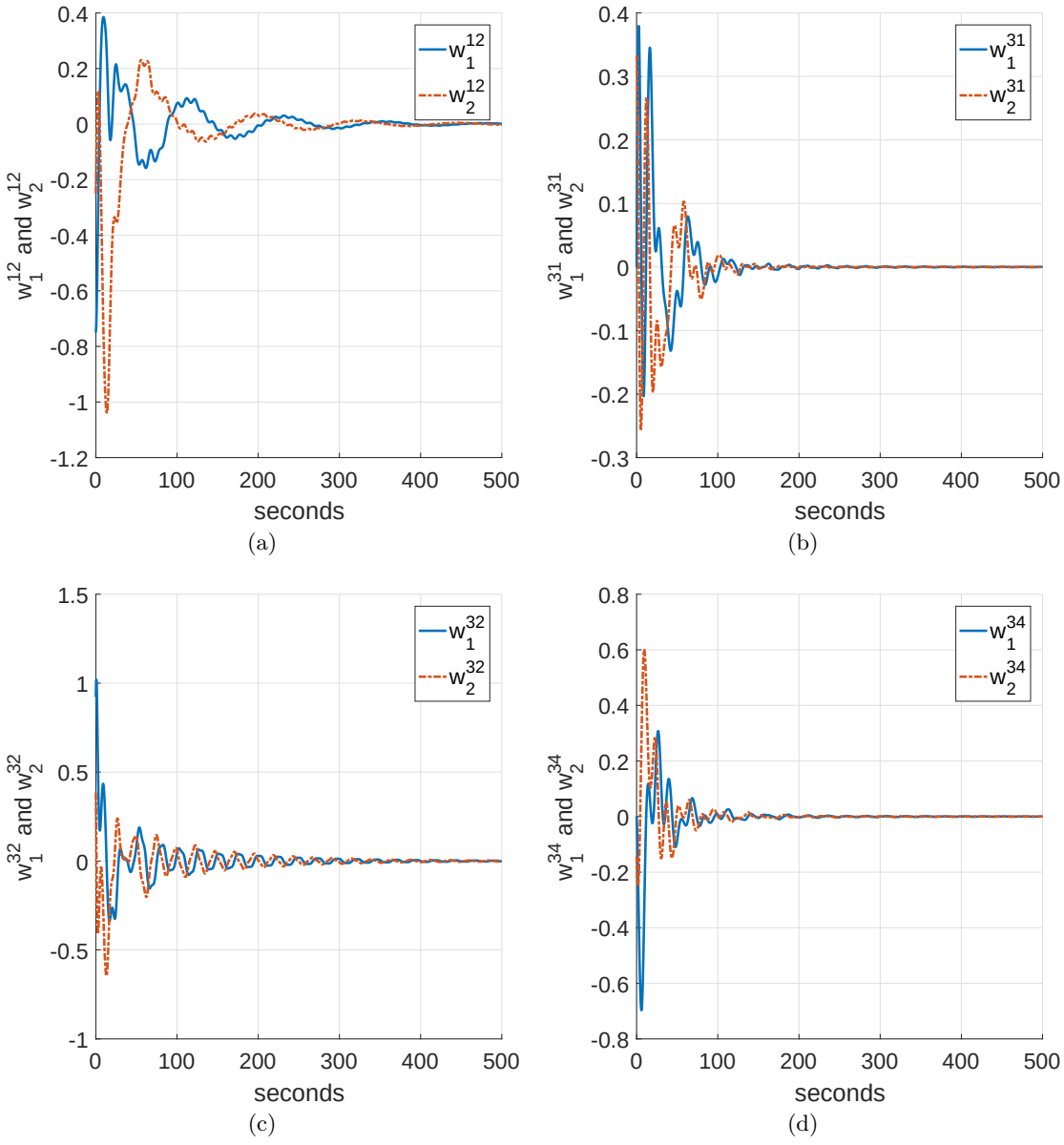

Figure 8: The w parameter state histories for Problem 2: (a) w parameters of spacecraft 2 in the frame of spacecraft 1; (b) w parameters of spacecraft 1 in the frame of spacecraft 3; (c) w parameters of spacecraft 2 in the frame of spacecraft 3; (d) w parameters of spacecraft 4 in the frame of spacecraft 3.

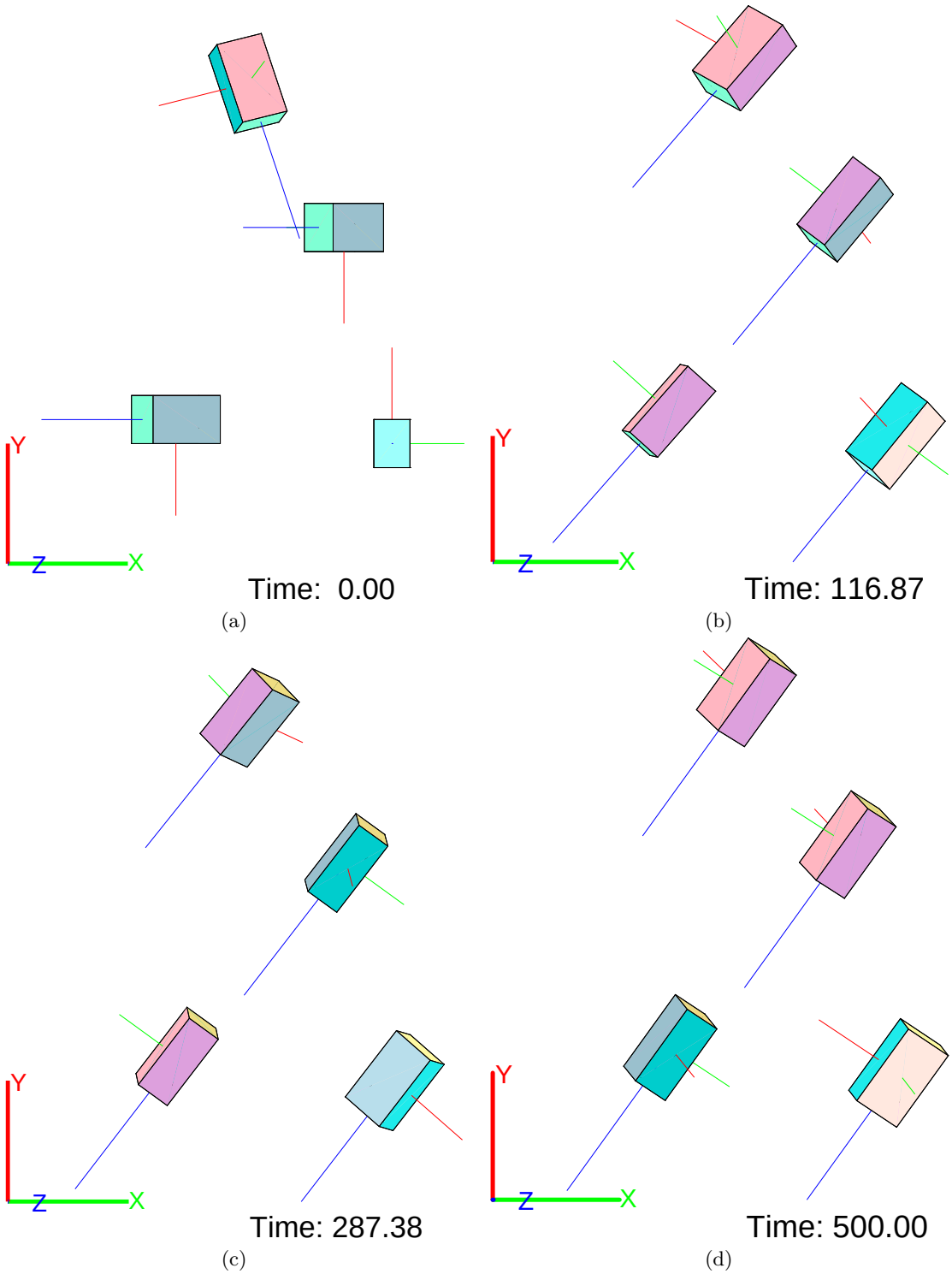

Figure 9: Snapshots at different phases of the simulation for Problem 2.

CHAPTER V

PARTIAL ATTITUDE SYNCHRONIZATION BETWEEN UNDERACTUATED SPACECRAFT TOWARDS A SPECIFIED FIXED INERTIAL DIRECTION

5.1 Introduction and Problem Definition

As mentioned in §1.3, most practical situations include a specific direction along which sensors need to point to. This chapter is dedicated to the extension of Problem 1 to a leader-follower scenario. Similar to what was assumed in Chapter 3, a network of multiple underacted spacecraft is considered with the goal of aligning their uncontrolled axes towards the same inertial direction, except for that one of the spacecraft possesses knowledge of a specific direction which is fixed in the inertial space. The objective for this chapter is then to have all spacecraft eventually point their uncontrolled axes towards a desired fixed inertial direction supplied to one of the spacecraft. This specified direction will, without loss of generality, be chosen to be the third axis of the inertial frame $\hat{\mathbf{b}}^d$. The reference direction is described in the frame of spacecraft i as $\hat{\mathbf{b}}_3^d = a^{id}\hat{\mathbf{b}}_1^i + b^{id}\hat{\mathbf{b}}_2^i + c^{id}\hat{\mathbf{b}}_3^i$, and the w parameters describing this reference direction in the frame of spacecraft i are $\mathrm{w}_1^{id} = b^{id}/(1+c^{id})$ and $\mathrm{w}_2^{id} = -a^{id}/(1+c^{id})$.

5.2 Main Result for Solving the Extension of Problem 1

Proposition 3. *Consider a network consisting of N spacecraft, and assume that the underlying communication graph $\mathcal{G}$ is a tree. The feedback control law*

$$\begin{bmatrix} u_1^i \\ u_2^i \end{bmatrix} = -\sum_{j\in\mathcal{N}_i} k_1^{ij}\mathrm{w}^{ij} - k_2^i\eta^i - k_4^i\mathrm{w}^{id}, \quad i \in \mathcal{V} \tag{51}$$

where the control gains are $k_1^{ij} = k_1^{ji} > 0$, $k_2^i > 0$ for all $i \in \mathcal{V}$, $k_4^\ell > 0$ for the leader $\ell \in \mathcal{V}$, and $k_4^i = 0$ for all $i \in \mathcal{V}\setminus\ell$, ensures that $\lim_{t\to\infty}\mathrm{w}^{id} = 0$ and $\lim_{t\to\infty}\eta^i = 0$ for all $i \in \mathcal{V}$, and thus solves the extension for Problem 1.

Proof. From the dynamics (21) and the control law (51), the closed-loop dynamics for each spacecraft $i \in \mathcal{V}$ is given by

$$\begin{aligned} I_1^i \dot{\omega}_1^i &= (I_2^i - I_3^i)\omega_2^i \omega_3^i - k_2^i \omega_1^i - k_4^i \mathrm{w}_1^{id} - \sum_{j \in \mathcal{N}_i} k_1^{ij} \mathrm{w}_1^{ij}, \\ I_2^i \dot{\omega}_2^i &= (I_3^i - I_1^i)\omega_1^i \omega_3^i - k_2^i \omega_2^i - k_4^i \mathrm{w}_2^{id} - \sum_{j \in \mathcal{N}_i} k_1^{ij} \mathrm{w}_2^{ij}, \\ I_3^i \dot{\omega}_3^i &= (I_1^i - I_2^i)\omega_1^i \omega_2^i. \end{aligned} \tag{52}$$

Consider the Lyapunov function candidate

$$V = \sum_{i \in \mathcal{V}} \sum_{j \in \mathcal{N}_i} \frac{1}{2} k_1^{ij} \ln(1 + \|\mathrm{w}^{ij}\|^2) + \sum_{i \in \mathcal{V}} \frac{1}{2} (\omega^i)^{\mathsf{T}} I^i \omega^i + k_4^\ell \ln(1 + \|\mathrm{w}^{\ell d}\|^2). \tag{53}$$

Taking the time derivative of V along the trajectories of the system (52) and using (25) yields

$$\begin{aligned} \dot{V} &= \sum_{i \in \mathcal{V}} \sum_{j \in \mathcal{N}_i} \frac{1}{2} k_1^{ij} \frac{2}{(1 + \|\mathrm{w}^{ij}\|^2)} (\mathrm{w}^{ij})^{\mathsf{T}} \dot{\mathrm{w}}^{ij} + \sum_{i \in \mathcal{V}} (\omega^i)^{\mathsf{T}} I^i \dot{\omega}^i + k_4^\ell \frac{2}{(1 + \|\mathrm{w}^{\ell d}\|^2)} (\mathrm{w}^{\ell d})^{\mathsf{T}} \dot{\mathrm{w}}^{\ell d} \\ &= -\sum_{i \in \mathcal{V}} k_2^i (\eta^i)^{\mathsf{T}} \eta^i - k_4^\ell (\eta^\ell)^{\mathsf{T}} \mathrm{w}^{\ell d} + k_4^\ell (\mathrm{w}^{\ell d})^{\mathsf{T}} \eta^\ell \\ &= -\sum_{i \in \mathcal{V}} k_2^i (\eta^i)^{\mathsf{T}} \eta^i \ \leq \ 0. \end{aligned} \tag{54}$$

It follows that the system is Lyapunov stable and hence the signals $\mathrm{w}^{\ell d}$, w^{ij} and ω^i for all $i \in \mathcal{V}$, $j \in \mathcal{N}_i$, are all bounded. From (52), it follows that $\mathcal{M} \triangleq \{(\mathrm{w}^{\ell d}, \eta^\ell), (\mathrm{w}^{ij}, \eta^i) : \dot{V} \equiv 0\} = \{(\mathrm{w}^{\ell d}, 0), (\mathrm{w}^{ij}, 0) : \sum_{j \in \mathcal{N}_i} k_1^{ij} \mathrm{w}^{ij} + k_4^i \mathrm{w}^{id} = 0, \ \forall i \in \mathcal{V}\}$.

Since an undirected tree with N vertices and $M = N - 1$ edges has an incidence matrix $\mathcal{D}(\mathcal{G}) \in \mathbb{R}^{N \times M}$ that is full column rank [16], the agreement subspace $\sum_{j \in \mathcal{N}_i} k_1^{ij} \mathrm{w}^{ij} + k_4^i \mathrm{w}^{id} = 0$ for all $i \in \mathcal{V}$ can be described as

$$\begin{bmatrix} \sum_{j \in \mathcal{N}_1} k_1^{1j} \mathrm{w}^{1j} \\ \vdots \\ \sum_{j \in \mathcal{N}_M} k_1^{Mj} \mathrm{w}^{Mj} \\ \sum_{j \in \mathcal{N}_N} k_1^{Nj} \mathrm{w}^{Nj} + k_4^N \mathrm{w}^{Nd} \end{bmatrix} = \mathbf{0} = \breve{\mathcal{D}}(\mathcal{G}) \breve{W}, \tag{55}$$

where $\breve{\mathcal{D}}(\mathcal{G}) \in \mathbb{R}^{2N \times 2N}$ is a block matrix constructed using (28) as

$$\breve{\mathcal{D}}(\mathcal{G}) = \begin{bmatrix} \tilde{\mathcal{D}}(\mathcal{G}) & \begin{bmatrix} 0_{2M} \\ \mathrm{I}_{2\times 2} \end{bmatrix} \end{bmatrix} \tag{56}$$

and where $\breve{W} \in \mathbb{R}^{2N}$ is a vector containing the w parameters constructed using (29) as

$$\breve{W} = \begin{bmatrix} W \\ k_4^N \mathrm{w}^{Nd} \end{bmatrix}. \tag{57}$$

In (55) we have taken $\ell \equiv N$ without loss of generality and the edges $\varepsilon_e \in \mathcal{E}$, $e = 1, \cdots, M$, have been directed such that the resulting graph forms an arborescence with vertex ℓ as its root.

It follows from Lemma 3, Lemma 2, and the fact that $\breve{\mathcal{D}}(\mathcal{G})$ is full rank that $\breve{W} = 0$ and $\mathrm{w}^{ij} = 0$ for all $i \in \mathcal{V}$, $j \in \mathcal{N}_i$. In addition, $\mathrm{w}^{\ell d} = 0$ and $\mathrm{w}^{ij} = 0$ for all $i \in \mathcal{V}$, $j \in \mathcal{N}_i$, implies that $\mathrm{w}^{id} = 0$ for all $i \in \mathcal{V}$. Thus, the agreement subspace $\mathcal{M}$ consists only of the point $\mathrm{w}^{id} = 0$ and $\eta^i = 0$ for all $i \in \mathcal{V}$. By LaSalle's invariance principle, the proof is complete. □

5.2.1 Simulation 3: Leader-Follower Extension to Proposition 1

For the leader-follower extension to Problem 1, the simulation for Problem 1 is modified so that the spacecraft represented by $i = 1$ serves as a reference direction, in which its attitude remains constant and no control torques act upon it. In this way, the spacecraft represented by $i = 3$ takes the role as the leader of the network (in which $\ell = 3$) due to its receipt of the reference direction from Spacecraft 1 in terms of an additional set of w parameters. We achieve this by assuming that the spacecraft communication topology is encoded in the sets $\mathcal{N}_i$, for $i \in \mathcal{V} = \{2, 3, 4\}$, where $\mathcal{N}_2 \triangleq \{3\}$, $\mathcal{N}_3 \triangleq \{2, 4\}$, $\mathcal{N}_4 \triangleq \{3\}$. The spacecraft are all underactuated so that the $\hat{\mathbf{b}}_3^i$ principal axis of each spacecraft $i \in \mathcal{V}$ is uncontrolled, and they possess moments of inertia $I^2 = \mathrm{diag}(15, 35, 45)$ kg $\cdot$ m^2, $I^3 = \mathrm{diag}(84, 24, 15)$ kg $\cdot$ m^2, and $I^4 = \mathrm{diag}(60, 40, 15)$ kg $\cdot$ m^2 for Spacecraft 2, 3, and 4, respectively. The initial orientations given in unit quaternions and the initial angular velocities for Spacecraft 1, 2, 3, and 4 were chosen as

$$q_1 = \begin{bmatrix} 0.6667 \\ -0.6667 \\ 0 \\ -0.3333 \end{bmatrix}, \quad q_2 = \begin{bmatrix} 0.5547 \\ 0.5547 \\ -0.2774 \\ 0.5547 \end{bmatrix}, \quad q_3 = \begin{bmatrix} 0 \\ -0.3162 \\ 0 \\ 0.9487 \end{bmatrix}, \quad q_4 = \begin{bmatrix} 0 \\ -0.4472 \\ 0 \\ 0.8944 \end{bmatrix}, \tag{58}$$

and

$$\omega^1(0) = \begin{bmatrix} 0 \\ 0 \\ 0 \end{bmatrix} \frac{\text{rad}}{\text{s}}, \quad \omega^2(0) = \begin{bmatrix} -0.1 \\ -0.1 \\ -0.2 \end{bmatrix} \frac{\text{rad}}{\text{s}}, \quad \omega^3(0) = \begin{bmatrix} 0.1 \\ 0.1 \\ 0.1 \end{bmatrix} \frac{\text{rad}}{\text{s}}, \quad \omega^4(0) = \begin{bmatrix} 0.1 \\ 0.3 \\ 0.1 \end{bmatrix} \frac{\text{rad}}{\text{s}}, \tag{59}$$

respectively, with the control gains set to $k_1 = 0.2$, $k_2^i = 1$ for $i = 2, 3, 4$, and $k_4^3 = 0.2$.

The w parameters describing the $\hat{\mathbf{b}}_3$ axis of Spacecraft 2 in the frame of the reference Spacecraft 1 and Spacecraft 1, 2, and 4 in the frame of Spacecraft 3 are plotted in Fig. 10. Similar behavior was observed for the other partial attitude parameters as well. In order to visually confirm the effectiveness of applying the control law to solve the extension of Problem 1, an animation from the simulation was created depicting the spacecraft as they rotate in inertial space, and several snapshots of various phases of the simulation are shown in Fig. 11.

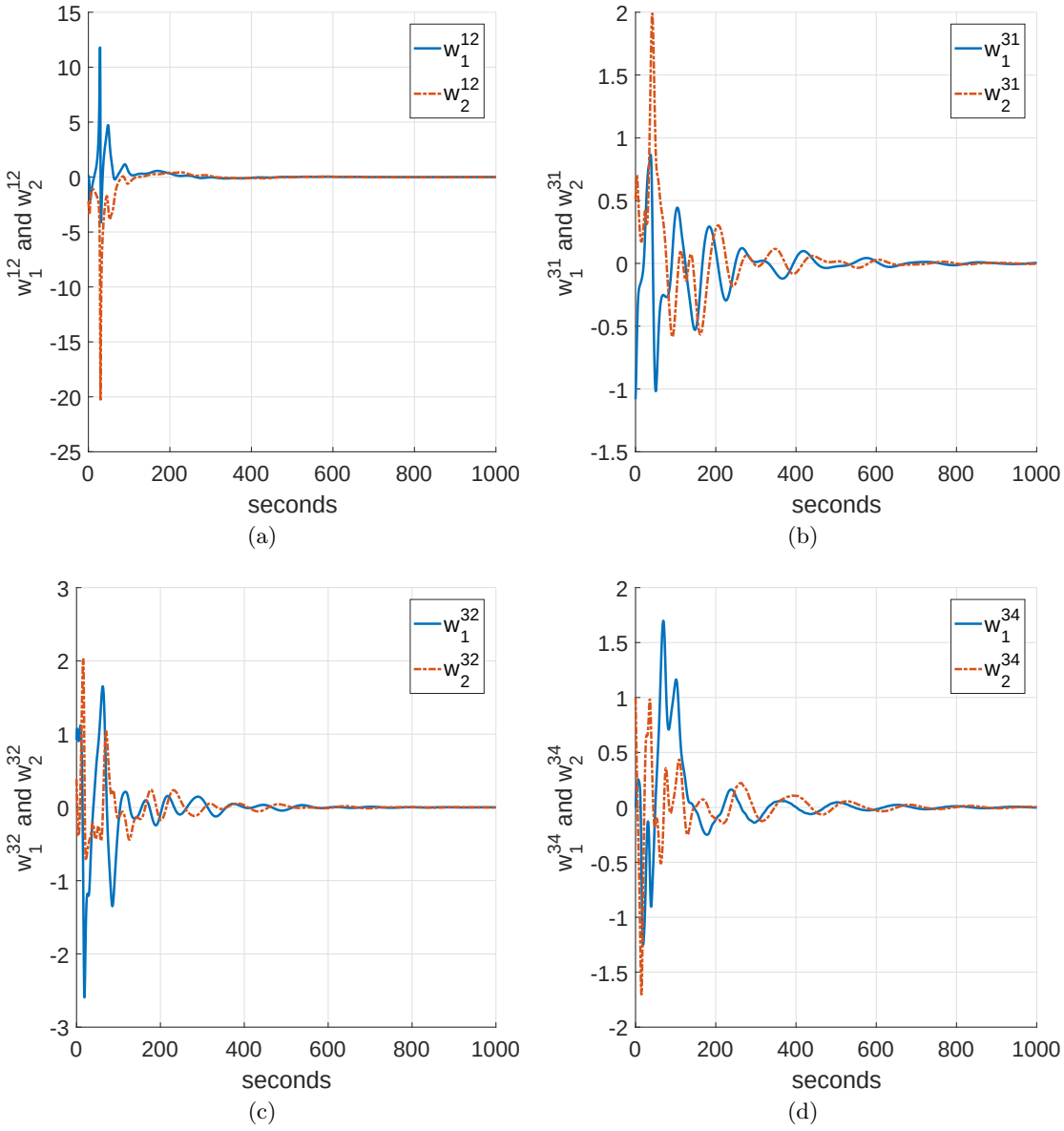

(a) (b) (c) (d)

Figure 10: The w parameter state histories for the extension to Problem 1: (a) w parameters of spacecraft 2 in the frame of spacecraft 1; (b) w parameters of spacecraft 1 in the frame of spacecraft 3; (c) w parameters of spacecraft 2 in the frame of spacecraft 3; (d) w parameters of spacecraft 4 in the frame of spacecraft 3.

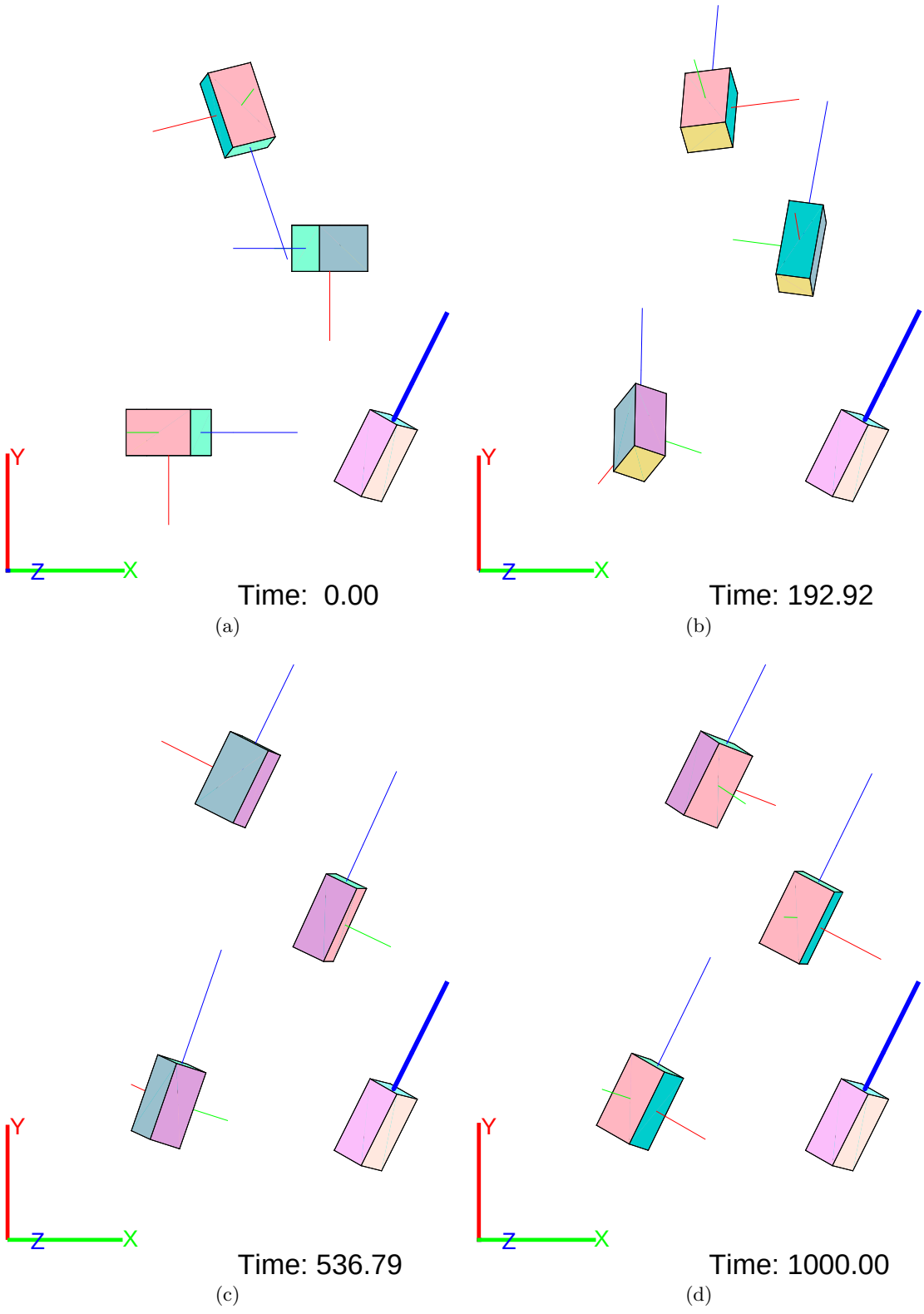

Figure 11: Snapshots at different phases of the simulation for the extension to Problem 1.

CHAPTER VI

CONCLUSION

6.1 Summary

Although there has been much work, especially in recent years, dealing with the attitude synchronization of multiple spacecraft and the control of single underactuated spacecraft, this is the first work that has successfully addressed the problem of partial attitude synchronization of multiple underactuated spacecraft, as far as the author knows.

In this thesis, two problems related to the partial attitude stabilization of multiple underactuated spacecraft were introduced, along with an extension. All problems focused on the control of multiple underactuated spacecraft, connected through a network, with the intention of aligning the uncontrolled axis of each spacecraft towards the same direction in inertial space. The first problem solved was the alignment of the uncontrolled axes towards a fixed unspecified inertial direction. The second problem solved was similar, but the final inertial direction was no longer necessarily fixed. The control law that solved it relied only upon relative state information of the neighboring spacecraft as opposed to inertial information, opening up the possibility to achieve partial synchronization of the spacecraft in the event of a failure or absence of communication when equipped with the appropriate sensors. Finally, an extension of the first problem to a leader-follower scenario was solved. It was shown that as long as the reference direction given to the leader of the network was fixed in inertial space, all spacecraft would point their uncontrolled axes towards it. Each solution guarantees almost global asymptotic stability of the partial consensus state.

6.2 Future Work

The work presented here opens many new possibilities for future investigation. As eluded to before, the solution of Problem 2 relies on the relative states of neighboring spacecraft, and therefore one possible avenue involves using a method, perhaps through onboard cameras for example, to capture the necessary relative information and demonstrate that the

stabilization of an underactuated spacecraft cluster is indeed possible without maintaining communication links. Since sensors are typically fixed on the spacecraft and the spacecraft considered here are free to rotate about their underactuated axis, the utilization of onboard sensors to acquire relative state information may involve periodic acquisition and absence of data, depending on the orientation of the sensors about the uncontrolled axis and the relative location of the neighboring spacecraft. Because of this, the idea of obtaining relative state information from onboard sensors may rely upon solving Problem 2 where the communication graph is modeled as being generally disconnected, directed, and switching. Additional avenues to explore include the generalization of the communication graphs for all problems to allow digraphs, dynamic structures, information lag, etc.; extending Problem 2 to a leader-follower scenario; and the incorporation of noisy measurements.

Extending these solutions to account for different graph structures is a particularly interesting topic since operating on the *Special Orthogonal Group* poses unique challenges. To demonstrate this, consider three spacecraft with the same dynamics as given in the problems presented before and whose underactuated axes are pointing 120° apart, and so exist in a plane. If each of the three spacecraft are communicating with the other two so that they are part of an undirected cycle, the control gains are the same, and inertial angular velocities zero about the controlled axes, then the summation term of the w parameters in the control laws proposed in Problem 1 and Problem 2 is zero, and so this state, while not the consensus desired as before, is an equilibrium point of the system. Besides cycles, switching communication topologies also affect systems operating in the Special Orthogonal Group differently than they would in Euclidean space. Consider the same spacecraft as before and let four of them exist, again, in a plane, with the uncontrolled axis of Spacecraft 1, 2, 3, and 4 pointing along the $+x$, $-x$, $+y$, and $-y$ directions, respectively, of some coordinate system with the axes x and y perpendicular to each other. Additionally, if the gains are equal and inertial angular velocities zero initially, and the communication graph contains the undirected edges $(1, 3)$ and $(2, 3)$ initially, then Spacecraft 1 and 2 would approach partial synchronization with Spacecraft 3. After some time before this synchronization, the communication topology may be switched so that the edges in the graph are now $(1, 4)$

and $(2, 4)$, causing the controls to resist synchronization between Spacecraft 1, 2, and 3, and attempting, instead, to partially synchronize Spacecraft 1, 2, and 4. In this scenario, the switching between these two graphs at the correct moments actually lead to a forever oscillating system.

The solution to other problems in the field of distributed multi-agent control may also benefit from the framework developed in this thesis. For instance, the formation control problem for underactuated spacecraft could involve the pointing of the uncontrolled axes so that a certain angular distance is maintained between them, instead of aligning them towards the same direction. Such a scenario may be advantageous when, for example, multiple spacecraft equipped with cameras are expected to capture a wide field of view, greater than the capabilities of a single camera, without inducing blind spots. This specific example also overlaps with the coverage problem, where a certain field of view or spherical polygon must be observed entirely.

REFERENCES

[1] Abdessameud, A., Ayebi, A., and Polushin, I. G., "Rigid body attitude synchonization with communication delays," in *American Control Conference*, (Montréal, Canada), pp. 3736–3741, June 27–29, 2012.

[2] Abdessameud, A. and Tayebi, A., "Attitude synchronization of a group of spacecraft without velocity measurements," *IEEE Transactions on Automatic Control*, vol. 54, pp. 2642–2648, Nov 2009.

[3] Bai, H., Arcak, M., and Wen, J. T., "Rigid body attitude coordination without inertial frame information," *Automatica*, vol. 44, no. 12, pp. 3170 – 3175, 2008.

[4] Bapat, R. B., *Graphs and Matrices*. Springer New York, 2014.

[5] Coron, J.-M. and Keraï, E.-Y., "Explicit feedbacks stabilizing the attitude of a rigid spacecraft with two control torques," *Automatica*, vol. 32, no. 5, pp. 669–667, 1996.

[6] de Queiroz, M. S., Kapila, V., and Yan, Q., "Adaptive nonlinear control of multiple spacecraft formation flying," *Journal of Guidance, Control, and Dynamics*, vol. 23, no. 3, pp. 385–390, 2000.

[7] Dimarogonas, D. V., Tsiotras, P., and Kyriakopoulos, K. J., "Laplacian cooperative attitude control of multiple rigid bodies," in *IEEE International Symposium on Intelligent Control*, (Munich, Germany), pp. 3064–3069, October 4-6 2006.

[8] Dimarogonas, D. V., Tsiotras, P., and Kyriakopoulos, K. J., "Leader-follower cooperative attitude control of multiple rigid bodies," *Systems & Control Letters*, vol. 58, no. 6, pp. 429 – 435, 2009.

[9] Erdong, J., Xiaolei, J., and Zhaowei, S., "Robust decentralized attitude coordination control of spacecraft formation," *Systems & Control Letters*, vol. 57, no. 7, pp. 567 – 577, 2008.

[10] Jeurissen, R., "The incidence matrix and labelings of a graph," *Journal of Combinatorial Theory, Series B*, vol. 30, no. 3, pp. 290 – 301, 1981.

[11] Kane, T. R., Likins, P. W., and Levinson, D. A., *Spacecraft Dynamics*. New York: McGraw-Hill Book Company, August 1983.

[12] Krishnan, H., McClamroch, N. H., and Reyhanoglu, M., "Attitude stabilization of a rigid spacecraft using two momentum wheel actuators," *Journal of Guidance, Control, and Dynamics*, vol. 18, no. 2, pp. 256–263, 1995.

[13] Lawton, J. R. and Beard, R. W., "Synchronized multiple spacecraft rotations," *Automatica*, vol. 38, no. 8, pp. 1359 – 1364, 2002.

[14] Ma, L., Min, H., Wang, S., Liu, Y., and Liao, S., "An overview of research in distributed attitude coordination control," *IEEE/CAA Journal of Automatica Sinica*, vol. 2, pp. 121–133, April 2015.

[15] Mathieu, C. and Weigel, A. L., "Assessing the flexibility provided by fractionated spacecraft," in *Space 2005*, (Long Beach, California), Aug. 30-Sep. 1, 2005.

[16] Mesbahi, M. and Egerstedt, M., *Graph Theoretic Methods in Multiagent Networks*. Princeton, New Jersey: Princeton University Press, 2010.

[17] Nair, S. and Leonard, N. E., "Stabilization of a coordinated network of rotating rigid bodies," in *43rd IEEE Conference on Decision and Control*, vol. 5, (Atlanta, GA), pp. 4690–4695, Dec. 15–17, 2004.

[18] Nair, S. and Leonard, N. E., "Stable synchronization of rigid body networks," *Networks and Heterogeneous Media*, vol. 2, no. 4, pp. 595–624, 2007.

[19] O'NEILL, M. G. and WEIGEL, A. L., "Assessing the impacts of fractionation on pointing-intensive spacecraft," in *SM Thesis, Aeronautics and Astronautics, Massachusetts Institute of Technology*, 2009.

[20] REN, W., "Distributed cooperative attitude synchronization and tracking for multiple rigid bodies," *IEEE Transactions on Control Systems Technology*, vol. 18, pp. 383–392, March 2010.

[21] SARLETTE, A., SEPULCHRE, R., and LEONARD, N. E., "Autonomous rigid body attitude synchronization," *Automatica*, vol. 45, no. 2, pp. 572 – 577, 2009.

[22] SHEN, H. and ROITHMAYR, C. M., "Co-spin with symmetry axis stabilization, and despin for asteroid capture," in *American Control Conference*, (Portland, OR), pp. 1599–1604, June 4–6, 2014.

[23] SHUSTER, M. D., "A survey of attitude representations," *The Journal of the Astronautical Sciences*, vol. 41, no. 4, pp. 439–517, 1993.

[24] TORCZYNSKI, D. M. and AMINI, R., "Magnetorquer based attitude control for a nanosatellite testplatform," in *AIAA Infotech@Aerospace*, (Atlanta, GA), April 20–22, 2010.

[25] TSIOTRAS, P., CORLESS, M. J., and LONGUSKI, J. M., "A novel approach to the attitude control of axisymmetric spacecraft," *Automatica*, vol. 31, no. 8, pp. 1099 – 1112, 1995.

[26] TSIOTRAS, P. and DOUMTCHENKO, V., "Control of spacecraft subject to actuator failures: State-of-the-art and open problems," *Journal of the Astronautical Sciences*, vol. 48, no. 2, pp. 337–358, 2000.

[27] TSIOTRAS, P. and LONGUSKI, J. M., "Spin-axis stabilization of symmetric spacecraft with two control torques," *Systems & Control Letters*, vol. 23, no. 6, pp. 395 – 402, 1994.

[28] Tsiotras, P. and Longuski, J. M., "A new parameterization of the attitude kinematics," *The Journal of the Astronautical Sciences*, vol. 43, no. 3, pp. 243–262, 1995.

[29] Tsiotras, P. and Longuski, J. M., "Comments on a new parameterization of the attitude kinematics," in *AIAA/AAS Astrodynamics Specialists Conference*, no. 3627 in 96, (San Diego, CA), AAS, July 29-31 1996.

[30] Tsiotras, P. and Luo, J., "Control of underactuated spacecraft with bounded inputs," *Automatica*, vol. 36, no. 8, pp. 1153 – 1169, 2000.

[31] Tsiotras, P. and Schleicher, A., "Detumbling and partial attitude stabilization of a rigid spacecraft under actuator failure," in *AIAA Guidance, Navigation, and Control Conference*, (Denver, CO), August 14–17, 2000.

[32] VanDyke, M. C. and Hall, C. D., "Decentralized coordinated attitude control within a formation of spacecraft," *Journal of Guidance, Control, and Dynamics*, vol. 29, no. 5, pp. 1101–1109, 2006.

[33] Wang, D., Jia, Y., Jin, L., and Xu, S., "Control analysis of an underactuated spacecraft under disturbance," *Acta Astronautica*, vol. 83, pp. 44 – 53, 2013.

[34] Wang, P. K. C., Hadaegh, F. Y., and Lau, K., "Synchronized formation rotation and attitude control of multiple free-flying spacecraft," *Journal of Guidance, Control, and Dynamics*, vol. 22, no. 1, pp. 28–35, 1999.

[35] Wie, B., *Space Vehicle Dynamics and Control*. Reston, VA: AIAA, Inc., Second ed., August 2008.

[36] Zhou, Z., "Spacecraft attitude tracking and maneuver using combined magnetic actuators," in *AIAA Guidance, Navigation and Control Conference*, (Toronto, Ontario Canada), August 2–5, 2010.